



Functional candesartan loaded lipid nanoparticles for the control of diabetes-associated stroke: In vitro *and* in vivo studies

Dina M. Mahmoud^a, Mohammed R.A. Ali^b, Basmah Nasser Aldosari^{c,*}, Randa Mohammed Zaki^{d,e}, Obaid Afzal^f, Alaa S. Tulbah^g, Demiana M. Naguib^h, Mohamed I. Zanatyⁱ, Mary Eskander Attia^j, Fatma I. Abo El-Ela^k, Amr Gamal Fouad^l

^a Department of Pharmaceutics, Faculty of Pharmacy, El Saleheya El Gadida University, El Saleheya El Gadida 44813, Sharkia, Egypt

^b Department of Pharmacology and Toxicology, Faculty of Pharmacy, Beni-Suef University, Beni-Suef, Egypt

^c Department of Pharmaceutics, College of Pharmacy, King Saud University, P.O. Box 2457, Riyadh 11451, Saudi Arabia

^d Department of Pharmaceutics, College of Pharmacy, Prince Sattam Bin Abdulaziz University, P.O. Box 173, Al-Kharj 11942, Saudi Arabia

^e Department of Pharmaceutics and Industrial Pharmacy, College of Pharmacy, Beni-Suef University, Beni-Suef 62514, Egypt

^f Department of Pharmaceutical Chemistry, College of Pharmacy, Prince Sattam Bin Abdulaziz University, P.O. Box 173, Al-Kharj 11942, Saudi Arabia

^g Department of Pharmaceutics, College of Pharmacy, Umm Al Qura University, Makkah, Saudi Arabia

^h Department of Pharmaceutics, Faculty of Pharmacy, Nahda University (NUB), Beni-Suef, Egypt

ⁱ Biotechnology and Life Science Department, Faculty of Postgraduate Studies for Advanced Sciences, Beni-Suef University, Egypt

^j Pharmacology Department, Faculty of Medicine, Beni-Suef University, Beni-Suef, Egypt

^k Department of Pharmacology, Faculty of Veterinary Medicine, Beni-Suef University, Beni-Suef, Egypt

^l Department of Pharmaceutics and Industrial Pharmacy, Faculty of Pharmacy, Beni-Suef University, Beni-Suef, Egypt

ARTICLE INFO

Keywords:

Diabetes mellitus
Stroke
Candesartan
Liposomes
Ethanol
Propylene glycol

ABSTRACT

Diabetes mellitus is a metabolic disease that raises the odds of developing stroke. Candesartan has been used to prevent stroke due to its inhibitory effects on blood pressure, angiogenesis, oxidative damage, and apoptosis. However, oral candesartan has very limited bioavailability and efficacy due to its weak solubility and slow release. The study aimed to develop a nasal formulation of candesartan-loaded liposomes containing ethanol and propylene glycol (CLEP) to improve candesartan's delivery, release, permeation, and efficacy as a potential diabetes-associated stroke treatment. Using design expert software, different CLEP formulations were prepared and evaluated in vitro to identify the optimum formulation, which.

The selected optimum formulation composed of 3.3% phospholipid, 10% ethanol, and 15% propylene glycol significantly increased the release and permeation of candesartan relative to free candesartan by a factor of 1.52 and 1.47, respectively. The optimum formulation significantly reduced the infarction after stroke in rats; decreased flexion, spontaneous motor activity, and time spent in the target quadrant by 70%, 64.71%, and 92.31%, respectively, and enhanced grip strength by a ratio of 2.3. Therefore, nasal administration of the CLEP formulation could be a potential diabetes-associated stroke treatment.

1. Introduction

Diabetes mellitus is a metabolic disease that occurs due to insulin

resistance, reduced glucose tolerance, and poor lipid and protein metabolism (Mosenzon et al., 2023; Tuttolomondo et al., 2015). Its complications raise the odds of developing cerebrovascular diseases

Abbreviations: CDT, Candesartan; EE%, Encapsulation efficiency; ANOVA, Analysis of variance; DSC, Differential Scanning Calorimetry; TEM, Transmission Electron Microscopy; R², Correlation coefficient; TG, Triglycerides; SD, Standard deviation; Q_{24h}, Cumulative percent CDT permeated after 24 h; Jss, Steady-state flux.

* Corresponding author.

E-mail addresses: doniadodododo@yahoo.com (D.M. Mahmoud), ragab_2000006@pharm.bsau.edu.eg (M.R.A. Ali), Baldosari@ksu.edu.sa (B.N. Aldosari), randazaki439@yahoo.com (R.M. Zaki), o.akram@psau.edu.sa (O. Afzal), astulbah@uqu.edu.sa (A.S. Tulbah), demiana.monier@nub.edu.eg (D.M. Naguib), Zanaty012@psas.bsau.edu.eg (M.I. Zanaty), Mary.eskandr@med.bsau.edu.eg (M.E. Attia), fatma.aboel3la@vet.bsau.edu.eg (F.I. Abo El-Ela), Amr_g@pharm.bsau.edu.eg (A.G. Fouad).

<https://doi.org/10.1016/j.ijpx.2023.100227>

Received 25 September 2023; Received in revised form 22 December 2023; Accepted 27 December 2023

Available online 2 January 2024

2590-1567/© 2023 The Author(s). Published by Elsevier B.V. This is an open access article under the CC BY-NC-ND license (<http://creativecommons.org/licenses/by-nc-nd/4.0/>).

such as ischemic stroke (Mosenzon et al., 2023; Policardo et al., 2015; Tuttolomondo et al., 2015). Stroke is a lack of blood flow to the brain as a result of thrombosis or embolism (Mosenzon et al., 2023; Policardo et al., 2015). Hyperglycemia contributes to the development of several risk factors for stroke, including atherosclerosis, cerebral small vessel disease, and cardiac embolism (Mosenzon et al., 2023; Policardo et al., 2015; Tuttolomondo et al., 2015). A stroke is a leading cause of adult disability and mortality globally (Mosenzon et al., 2023; Policardo et al., 2015; Tuttolomondo et al., 2015).

Multiple studies have demonstrated the efficacy of anti-hypertensive medication in preventing diabetes-related stroke (Hägg-Holmberg et al., 2019; Lawes et al., 2004). Candesartan (CDT) is a type of oral angiotensin II receptor antagonist that has been licensed for the treatment of cerebrovascular insufficiency and peripheral vascular disease. Due to its inhibitory effects on blood pressure, inflammation, angiogenesis, oxidative damage, and apoptosis, CDT has been used to prevent stroke (Ding et al., 2022; Kozak et al., 2009; Nishimura et al., 2000; Zhou et al., 2006). Also, it enhances insulin sensitivity by better delivering insulin and glucose to peripheral skeletal muscle (Nakao et al., 2010). However, oral CDT has very limited bioavailability due to its weak water solubility and slow dissolution rate (Aly et al., 2020; Dudhipala and Veerabrahma, 2016; Zhang et al., 2012a, 2012b). Hepatic first-pass degradation also contributes to CDT's poor absorption (Aly et al., 2020; Khawaja and Wilcox, 2011).

Nasal administration as an alternative to oral administration has been investigated due to the high vascularity of the nasal mucosa, rapid onset of action and absence of first-pass metabolism (Cunha et al., 2017; Fasiolo et al., 2018). In addition, the olfactory receptor cells are in direct contact with the central nervous system, making nasal medication delivery a noninvasive option for the direct delivery of drugs to the brain (Wang et al., 2013). However, nasal delivery has various challenges due to the formulation's short residence time within the nasal cavity and the drug's limited permeability (Cunha et al., 2017; Fasiolo et al., 2018; Wang et al., 2013). To counteract these limitations, lipid-based nanoparticles could be used to improve drug permeability and lessen mucociliary clearance (Cunha et al., 2017; Salem et al., 2021).

Liposomes, which are a combination of phospholipids and cholesterol, are ideal drug delivery carriers because of their high diffusion coefficients and specificity (Gamal et al., 2021; Salem et al., 2021). Due to their increased solubility and release through cellular membranes, liposomes can increase the drug's bioavailability and effectiveness (Gamal et al., 2021; Salem et al., 2021). The presence of phospholipids and cholesterol increases the viscosity of formulations, which in turn reduces the mucociliary clearance. Drug leakage and poor vesicle stability and permeability are problems associated with liposomes; hence, penetration enhancers such as propylene glycol and ethanol have been added (Abdulbaqi et al., 2016; Zhang et al., 2012a, 2012b).

Ethanol is a powerful penetration enhancer because it softens the vesicles, which lets them able to traverse the nasal epithelium, and makes the vesicles smaller and increases their surface area and ability to absorb (Touitou et al., 2000; Abdulbaqi et al., 2016). Propylene glycol is a widely used penetration enhancer that makes the drug permeates into the skin more easily (Zhang et al., 2012a, 2012b; Salem et al., 2021). As it is more viscous and hygroscopic than ethanol, propylene glycol may increase vesicle affinity for molecules in the water-based dermis layer, slowing the vesicles' transit through the skin and increasing their concentration in the deep skin (Shen et al., 2014). When ethanol and propylene glycol combine, they increase the skin's fluidity (Zhang et al., 2012a, 2012b; Abdulbaqi et al., 2016). Additionally, ethanol increases the stability of the liposomes and inhibits the vesicles from clustering due to electrostatic repulsion (Abdulbaqi et al., 2016; Gamal et al., 2021). Propylene glycol increases the stability of the liposomes by increasing the viscosity of vesicular formulations (Zhang et al., 2012a, 2012b).

To our knowledge, there have been no studies that have developed CDT-loaded liposomes containing ethanol and propylene glycol (CLEP)

nanovesicles to improve the delivery, release, permeability, and efficacy of CDT. Various studies have utilized liposomes containing ethanol and propylene glycol nanovesicles for transdermal drug delivery. However, our research focused on the possibility of using CLEP nanovesicles as nasal drops to treat cerebrovascular diseases like stroke. Thus, the purpose of this study was to improve CDT's delivery, release, permeation, and efficacy as a potential diabetes-associated stroke treatment by developing a nasal formulation of CLEP. The release, permeation and anti-stroke effectiveness of CDT can be improved through the production of a nasal CLEP formulation by increasing nasal retention time, permeation, and release. Using design expert software, different CLEP formulations were prepared and characterized in vitro to identify the optimum formulation, which was then evaluated in vivo on an experimental diabetes and stroke rat model.

2. Materials and methods

2.1. Materials

Candesartan was provided by AstraZeneca, a pharmaceutical Company of Egypt. Phospholipid (L- α -phosphatidylcholine), tween 80 (polysorbate 80), potassium dihydrogen phosphate, disodium hydrogen phosphate, cholesterol, and propylene glycol were purchased from Agitech Company (Cairo, Egypt). Methanol, ethanol, and chloroform were purchased from Cornell Lab Company (Cairo, Egypt).

2.2. Experimental design

For the purpose of statistical optimization of CDT-loaded liposomes containing ethanol and propylene glycol (CLEP), a 3^3 Box-Behnken design was implemented (Table 1) using design expert software (Version 12, Stat-Ease Inc. Minneapolis, MN, USA). We evaluated the impacts of three variables: (A) L- α -phosphatidylcholine concentration (1–5%), (B) ethanol concentration (0–10%) and (C) propylene glycol concentration (5–15%). Particle size and encapsulation efficiency as a percentage (EE%) were selected as dependent variables.

2.3. Preparation of CLEP formulations

Fifteen different CLEP formulations were made using the thin-film hydration technique (Salem et al., 2022). Cholesterol (0.16%), L- α -phosphatidylcholine, CDT (10 mg), and propylene glycol were dissolved in 10 mL of chloroform-methanol solution at a ratio of 3:1 after being weighed. Using a rotary evaporator (Rotavapor, Heidolph VV

Table 1
Compositions and responses of CLEP formulations.

Run	Factors levels in actual values			Responses (n = 3)	
	A (%)	B (%)	C (%)	Encapsulation efficiency (% \pm SD)	Particle size (nm \pm SD)
F1	3	5	10	74.05 \pm 0.42	236.03 \pm 6.05
F2	5	10	10	90.65 \pm 0.39	386.20 \pm 4.17
F3	3	5	10	74.14 \pm 0.37	231.70 \pm 7.35
F4	3	0	5	69.17 \pm 0.41	279.47 \pm 6.83
F5	5	5	5	85.81 \pm 0.45	422.03 \pm 7.95
F6	3	5	10	74.10 \pm 0.40	230.70 \pm 4.00
F7	1	0	10	57.59 \pm 0.49	213.40 \pm 3.30
F8	5	5	15	88.47 \pm 0.35	389.83 \pm 5.65
F9	3	10	5	76.34 \pm 0.39	219.67 \pm 4.16
F10	1	10	10	65.08 \pm 0.36	159.60 \pm 4.65
F11	3	0	15	71.79 \pm 0.32	247.23 \pm 3.96
F12	1	5	15	62.54 \pm 0.37	169.43 \pm 9.71
F13	5	0	10	83.50 \pm 0.32	442.70 \pm 4.33
F14	3	10	15	79.31 \pm 0.45	187.83 \pm 3.25
F15	1	5	5	60.16 \pm 0.42	196.63 \pm 6.89

A: L- α -phosphatidylcholine concentration, B: ethanol concentration, C: propylene glycol concentration; SD: standard deviation.

2000, Burladingen, Germany) under vacuum at 100 rpm and 40 °C, the organic phase was evaporated until a thin, dry film formed and the organic odor disappeared. A phosphate buffer (pH 6.8) containing ethanol was used to hydrate the dried thin film. During the hydration process, the film was rotated and heated at 60 rpm and 60 °C for 2 h. The CLEP suspension was kept at 4 °C.

2.4. Characterization of CLEP formulations

2.4.1. Measurement of encapsulation efficiency

In order to determine the CLEP's encapsulation efficiency, we centrifuged the CLEP suspension at 15000 rpm and 4 °C for 2 h in a cooling centrifuge (SIGMA 3–30 K, Steinheim, Germany). To achieve complete separation of the CLEP pellets, we re-centrifuged the supernatant at 15,000 rpm for 1 h. An aliquot of the clear supernatant was diluted appropriately, and the CDT concentration was then determined by spectrophotometry (UV-1850, Shimadzu Corporation, Kyoto, Japan) at 258 nm in accordance with a standard calibration curve. The EE% of CDT was calculated as follows (Gamal et al., 2020):

$$EE\% = \frac{\text{Initial amount of CDT} - \text{amount of CDT in supernatant}}{\text{Initial amount of CDT}} \times 100 \quad (1)$$

2.4.2. Measurement of particle size

In order to determine the CLEP's particle size, we diluted a sample of CLEP suspension (1 mL) with distilled water (9 mL) and the size was measured in triplicate at 25 °C using dynamic light scattering with Zeta Sizer equipment (DLS, Malvern Instruments/Herrenberg, Germany) (El-Ela et al., 2022).

2.5. Optimization of CLEP formulations

To determine which model is most appropriate for the given EE% and particle size data, design expert® software applies the statistical methods such as analysis of variance (ANOVA), coefficient of determination (R^2), Adjusted R^2 , Predicted R^2 and Adequate precision (Sayed et al., 2020). Further, the desirability index is calculated so that the optimum formulation with the highest EE% and smallest particle size can be selected. A triple batch of the software's recommended formulation was prepared and assessed to confirm the correctness of its optimum formulation factor estimates and expected responses.

2.6. Characterization of optimum CLEP formulation

2.6.1. Differential scanning calorimetry (DSC)

Using DSC, we looked into how CDT and other components of optimum CLEP formulation interact with one another (Salem et al., 2021). The crystalline properties and thermal analysis (ΔH) of the CDT, L- α -phosphatidylcholine, cholesterol, and the optimum CLEP formulation were investigated using DSC. Samples of CDT, L- α -phosphatidylcholine, cholesterol, and optimum CLEP formulation were accurately weighed into sealed aluminum pans, and the experiment was conducted using DSC (Shimadzu DSC60 plus, Shimadzu Corporation, Kyoto, Japan) under nitrogen gas (50 ml/min) at a rate of 5 °C/min from 25 °C and 250 °C.

2.6.2. Fourier transform infrared (FT-IR) spectroscopy

FTIR analysis was utilized to gather evidence on the potential CDT interaction with other components of optimum CLEP formulation (Gamal et al., 2023). The potassium bromide disc method was used to prepare CDT, cholesterol, L- α -phosphatidylcholine and the optimum CLEP formulation samples (2 mg of sample in 200 mg of KBR) and the scanning range was set to be 400–4000 cm^{-1} using an FT-IR emission spectrometer (Shimadzu FTIR-8700 spectrophotometer, Shimadzu, Japan).

2.6.3. Transmission electron microscopy (TEM)

Using TEM, we looked into the morphology and size of the optimum CLEP formulation (Sayed et al., 2020). We used phosphotungstic acid dye to stain an aliquot of CLEP suspension that had been put onto a carbon covered grid and the experiment was conducted using transmission electron microscopy (JEM-1230 Scanning microscope, Jeol, Tokyo, Japan).

2.6.4. Zeta potential and size distribution

Using zeta potential and polydispersity index (PDI), we assessed the stability and homogeneity of the optimum CLEP formulation, respectively (El-Ela et al., 2022). Prior to the measurement, we diluted a sample (1 mL) of the optimum CLEP suspension with distilled water (9 mL) and the zeta potential and PDI were measured in triplicate at 25 °C using dynamic light scattering with Zeta Sizer equipment (DLS, Malvern Instruments/Herrenberg, Germany).

2.6.5. Stability study

Stability of CLEP formulation was studied by looking at how the formulation changed in terms of particle size and EE% (Gamal et al., 2021). CLEP Formulations were kept for three months at a temperature of 4 °C in the refrigerator, 25 °C at room temperature and 40 °C in the oven (Dental – UND LABORBAU GmbH 99,830 Treffurt/Germany). Once a month, three replicate measurements were analyzed for particle size and EE%.

2.6.6. In vitro release study

Using the dialysis membrane technique, we investigated the release of optimum CLEP formulation in comparison to free CDT (Salem et al., 2022). A volume of free CDT and CLEP equivalent to 2 mg of CDT was enclosed in a dialysis bag (molecular weight cut off 12,000; Sigma-Aldrich, Cairo, Egypt) and immersed into 50 mL of phosphate-buffered (pH 6.8) containing 0.1% (w/w) Tween 80 as a release medium at 100 rpm and 37 °C using Hanson dissolution apparatus (Hilab, Düsseldorf, Germany). 3 mL samples were taken and replaced with fresh medium at 0, 5, 1, 2, 3, 4, 6, 8 and 24 h. The CDT concentration was then determined by spectrophotometry (UV-1850, Shimadzu Corporation, Kyoto, Japan) at 258 nm in accordance with a standard calibration curve and the cumulative release percentage was calculated in triplicates.

2.6.7. Ex vivo permeation study

The nasal cavity of a freshly sacrificed Egyptian sheep was acquired, excluding the septum, and soaked in phosphate buffer for 24 h. The superior nasal membrane was excised and used to investigate the permeation of optimum CLEP formulation in comparison to free CDT (Salem et al., 2022). A volume of free CDT and CLEP equivalent to 2 mg of CDT was immersed into 50 mL of phosphate-buffered (pH 6.8) containing 0.1% (w/w) Tween 80 at 100 rpm and 37 °C using Hanson dissolution apparatus (Hilab, Düsseldorf, Germany). 3 mL samples were taken and replaced with fresh medium at 0, 5, 1, 2, 3, 4, 6, 8 and 24 h. The CDT concentration was then determined by spectrophotometry (UV-1850, Shimadzu Corporation, Kyoto, Japan) at 258 nm in accordance with a standard calibration curve and the cumulative permeation percentage and flux were calculated in triplicates.

2.7. In vivo evaluation of optimum CLEP formulation

2.7.1. Study design

In vivo studies of CLEP formulation were conducted in accordance with the ARRIVE guidelines and approved by the Institutional Animal Ethics Committee at Beni-Suef University (BSU-IACUC: 022–414).

2.7.2. Animals

Twenty four adult male Wistar rats (150–200 g body weight, 2–3 months old) were housed in the animal house (Faculty of Pharmacy, Beni-Suef University, Egypt) in air-conditioned clean polypropylene

cages (temperature of 25 °C and humidity of 40–70%). Prior the experiment, rats were acclimated for a week and fed with standard diet and water. Body weight, blood glucose, triglyceride (TG), cholesterol, red blood cell (RBC) count, white blood cell (WBC) count, alanine aminotransferase (ALT), aspartate aminotransferase (AST), urea, and creatinine levels were established for each rat.

2.7.3. Stroke induction and treatment administration

After acclimating for a week, the rats were randomly divided into two groups: a control negative group ($n = 6$ rats) and an ischemic stroke group ($n = 18$ rats). A control group ($n = 6$ rats) received intraperitoneal injection of 0.9% saline solution and continued to eat normally throughout the research. An ischemic stroke group ($n = 18$ rats) received high-fat diets containing cholesterol (6%), sodium cholate (1%), propyl thiouracil (0.2%), and refined sugar (5%) to induce diabetes and atherosclerosis and speed up the progression of an experimental model of ischemic stroke (Lian et al., 2018; Pérez-Corredor et al., 2022). After 12 weeks, an ischemic stroke group ($n = 18$ rats) were subdivided into three groups (6 rats each, positive control, free CDT and CLEP groups). A positive control group ($n = 6$ rats) received a daily oral gavage of 0.9% saline solution. A free CDT group ($n = 6$ rats) received a daily oral gavage of free CDT (1 mg/kg) (Kozak et al., 2009). A CLEP group ($n = 6$ rats) received a daily nasal administration of CLEP (1 mg/kg). After 10 days of treatments, the positive control, free CDT and CLEP groups were injected intraperitoneally with a mixture (1:1) of ketamine (90 mg/kg) and xylazine (5 mg/kg) at a concentration of 0.1 ml/100 g to induce anesthesia. Ischemic stroke was induced by blocking the main blood supply to the brain by occluding the common carotid and middle cerebral arteries with an intraluminal suture (Ashafaq et al., 2021). The rats' weight and behavior were monitored and documented during the trial (Kumar et al., 2017).

2.7.4. Neurological function assessment

At the end of experiment, neurological tests on the negative control, positive control, free CDT and CLEP groups, including grip strength, flexion, spontaneous motor activity, and Morris water maze, were conducted. The neurological deficits were scored on a point scale system (Zhao et al., 2020; Ashafaq et al., 2021).

As described by Ashafaq et al., the grip strength test was used to assess motor deficits of rats by placing the rat's paws on a wire grid while its tail was pulled backwards and the Morris water maze test was used to assess its memory impairments by calculating the time spent in the target quadrant (Ashafaq et al., 2021).

As described by Tabassum et al., the flexion test was used to measure the rat's ability to flex towards the ground while the rat was held upside down by its tail and the spontaneous motor activity was used to assess the neurological indices (Tabassum et al., 2013).

2.7.5. Histopathology study

After assessment of neurological tests, the experimental groups were euthanized by cervical dislocation after being injected intraperitoneally with a mixture (1:1) of ketamine (90 mg/kg) and xylazine (5 mg/kg) at a concentration of 0.1 ml/100 g. The blood was drawn, centrifuged, and the serum cholesterol, triglycerides, and glucose levels were assessed as directed by the manufacturer to confirm the successful production of diabetes and atherosclerosis (Ekeanyanwu and Njoku, 2014; Kumar et al., 2017).

Brain tissues were collected and fixed in 10% phosphate-buffered formalin. Tissues were cleaned in xylene, dehydrated in a graded ethanol solution, and then embedded in paraffin. Thin slices of tissue (4–6 μm) were prepared and stained using hematoxylin and eosin reagents in accordance with standard protocol (Ekeanyanwu and Njoku, 2014).

2.7.6. Toxicity studies

The rats' weight and behavior were monitored and documented

during the trial (Kumar et al., 2017). The serum RBCs ($\times 1000^3/\mu$) count, WBCs ($\times 10^3/\text{mm}^3$) count, hemoglobin (Hb, g/dl), hematocrit (HCT, %), Mean corpuscular volume (MCV, fl/cell), Mean Corpuscular Hemoglobin (MCH, pg/cell), neutrophils, lymphocytes, monocytes, eosinophils, basophils ALT, AST, urea and creatinine were assessed as directed by the manufacturer to evaluate the toxicity issues of nasal CLEP formulation (Ekeanyanwu and Njoku, 2014; Kumar et al., 2017).

2.8. Statistical analysis

SPSS (version 22, Chicago, USA) was used to conduct statistical analysis of the data using the Student's *t*-test and analysis of variance (ANOVA) followed by Tukey's post hoc for pairwise comparisons. A difference between study groups is considered significant at a *p*-value < 0.05 .

3. Results

3.1. Experimental design

Successful CLEP formulations were prepared and optimized using the Box-Behnken design. The quadratic model was the best fit for the EE% and particle size data because it had the highest determination coefficient (R^2) of 0.9989 and 0.9970, respectively, an insignificant lack-of-fit with *p*-values of 0.8584 and 0.5188, respectively, and a significant model with *p*-value of < 0.0001 . Close agreement (< 0.2) between the predicted (0.9981 and 0.9950) and adjusted R^2 (0.9986 and 0.9962) values further verified the quadratic model's validity for both EE% and particle size, respectively. The high values of adequate precision (188.949 and 105.612) confirmed the suitability of the quadratic model for both EE% and particle size, respectively for design space tracking. The diagnostic charts used to assess the quadratic model fit are depicted in Fig. 1. The Box-Cox plot (Fig. 1a and c) showed that the recommended value of lambda (λ) for both EE% and particle size is 1.15, suggesting that their data did not require any transformation. The Residuals vs predicted response plot (Fig. 1b and d) showed a random scatter, suggesting no continuous error (transformation) of both EE% and particle size data.

3.2. Characterization of CLEP formulations

The response surface plot for the effects of L- α -phosphatidylcholine, ethanol, and propylene glycol concentrations as independent variables on the EE% and particle size is depicted in Fig. 2 and represented by Eqs. (2) and (3) in terms of coded values. L-phosphatidylcholine concentration (A) had a statistically significant (*p*-value of < 0.0001) positive effect on EE%, where EE% of F10 (formulation with 1% L-phosphatidylcholine) and F2 (formulation with 5% L-phosphatidylcholine) was $65.08 \pm 0.36\%$ and $90.65 \pm 0.39\%$, respectively. Ethanol concentration (B) had a statistically significant (*p*-value of < 0.0001) positive effect on EE%, where EE% of F4 (formulation with 0% ethanol) and F9 (formulation with 10% ethanol) was $69.17 \pm 0.41\%$ and $76.34 \pm 0.39\%$, respectively. Propylene glycol concentration (C) had a statistically significant (*p*-value of < 0.0001) positive effect on EE%, where EE% of F5 (formulation with 5% propylene glycol) and F8 (formulation with 15% propylene glycol) was $85.81 \pm 0.45\%$ and $88.47 \pm 0.35\%$, respectively.

$$EE\% = +74.10 + 12.88A + 3.67B + 1.33C - 0.0839AB + 0.0702AC + 0.0873BC + 0.1A^2 + 0.0109B^2 + 0.0449C^2 \quad (2)$$

L-phosphatidylcholine concentration (A) had a statistically significant (*p*-value of < 0.0001) positive effect on particle size, where particle size of F7 (formulation with 1% L-phosphatidylcholine) and F13 (formulation with 5% L-phosphatidylcholine) was 213.40 ± 3.30 nm and 442.70 ± 4.33 nm, respectively. Ethanol concentration (B) had a

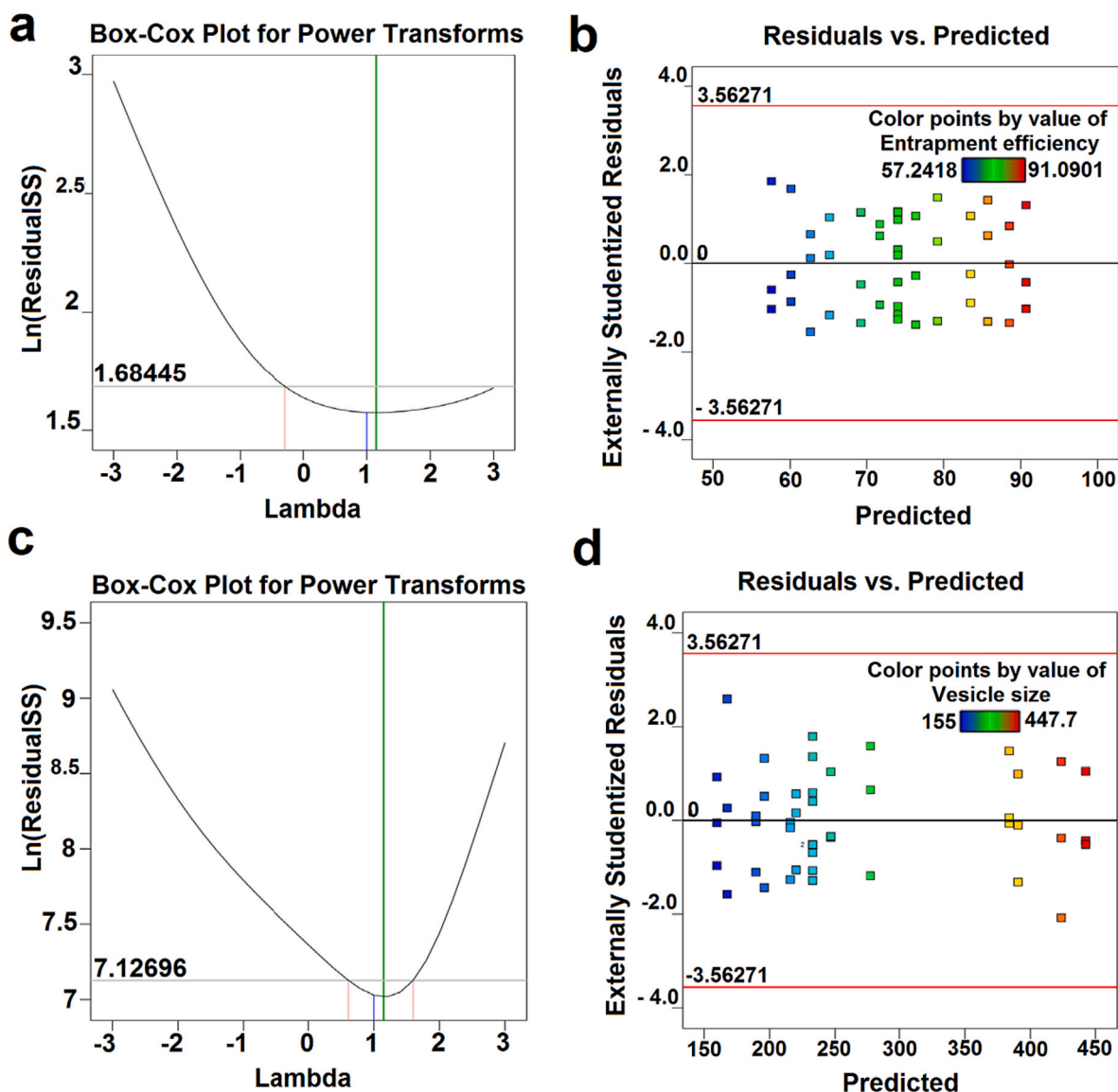


Fig. 1. Diagnostic plot of CLEP formulations; (a) and (c) Power transforms Box–Cox plot; the value of lambda is used to select a model power transform by plotting the data in a Box–Cox plot. (b) and (d) Studentized residuals vs. predicted response plot for EE% and particle size, respectively. Residual vs. predicted response provides a visual representation of the distribution of the measured response.

statistically significant (p -value of <0.0001) negative effect on particle size, where particle size of F11 (formulation with 0% ethanol) and F14 (formulation with 10% ethanol) was 247.23 ± 3.96 nm and 187.83 ± 3.25 nm, respectively. Propylene glycol concentration (C) had a statistically significant (p -value of <0.0001) negative effect on particle size, where particle size of F9 (formulation with 5% propylene glycol) and F14 (formulation with 15% propylene glycol) was 219.67 ± 4.16 nm and 187.83 ± 3.25 nm, respectively.

$$\begin{aligned} \text{Particle size} = & +232.81 + 112.71A - 28.69B - 15.43C - 0.675AB - 1.25AC \\ & + 0.1BC + 64.3A^2 + 3.37B^2 - 2.63C^2 \end{aligned} \quad (3)$$

3.3. Optimization of CLEP formulation

Based on its high desirability index (0.761), the formulation with 3.3%w/v phospholipid, 10%v/v ethanol, 0.16%w/v cholesterol, and 15%v/v propylene glycol was chosen as the optimum formulation. Predicted values of responses were verified by in vitro studies of the

optimum CLEP formulation, with an EE% of $81.13 \pm 0.52\%$ and a mean particle size of 207.26 ± 5.89 nm.

3.4. Characterization of optimum CLEP formulation

3.4.1. Differential scanning calorimetry (DSC)

DSC thermograms of CDT, cholesterol, L- α -phosphatidylcholine, and optimum CLEP formulation are shown in Fig. 3(a). CDT is a crystalline drug, showing a sharp endothermic peak at its melting point of 171.91 °C with ΔH of -49.15 J/g. Cholesterol showed a sharp endothermic peak at its melting point of 149.47 °C with ΔH of -109.69 J/g. L- α -phosphatidylcholine showed a sharp endothermic peak at its melting point of 134.96 °C with ΔH of -45.19 J/g. These endothermic peaks disappeared in the DSC thermogram of the optimum CLEP formulation.

3.4.2. Fourier transform infrared (FTIR)

The FTIR spectra of CDT, L- α -phosphatidylcholine, cholesterol, and an optimum CLEP formulation are shown in Fig. 3(b). The L-

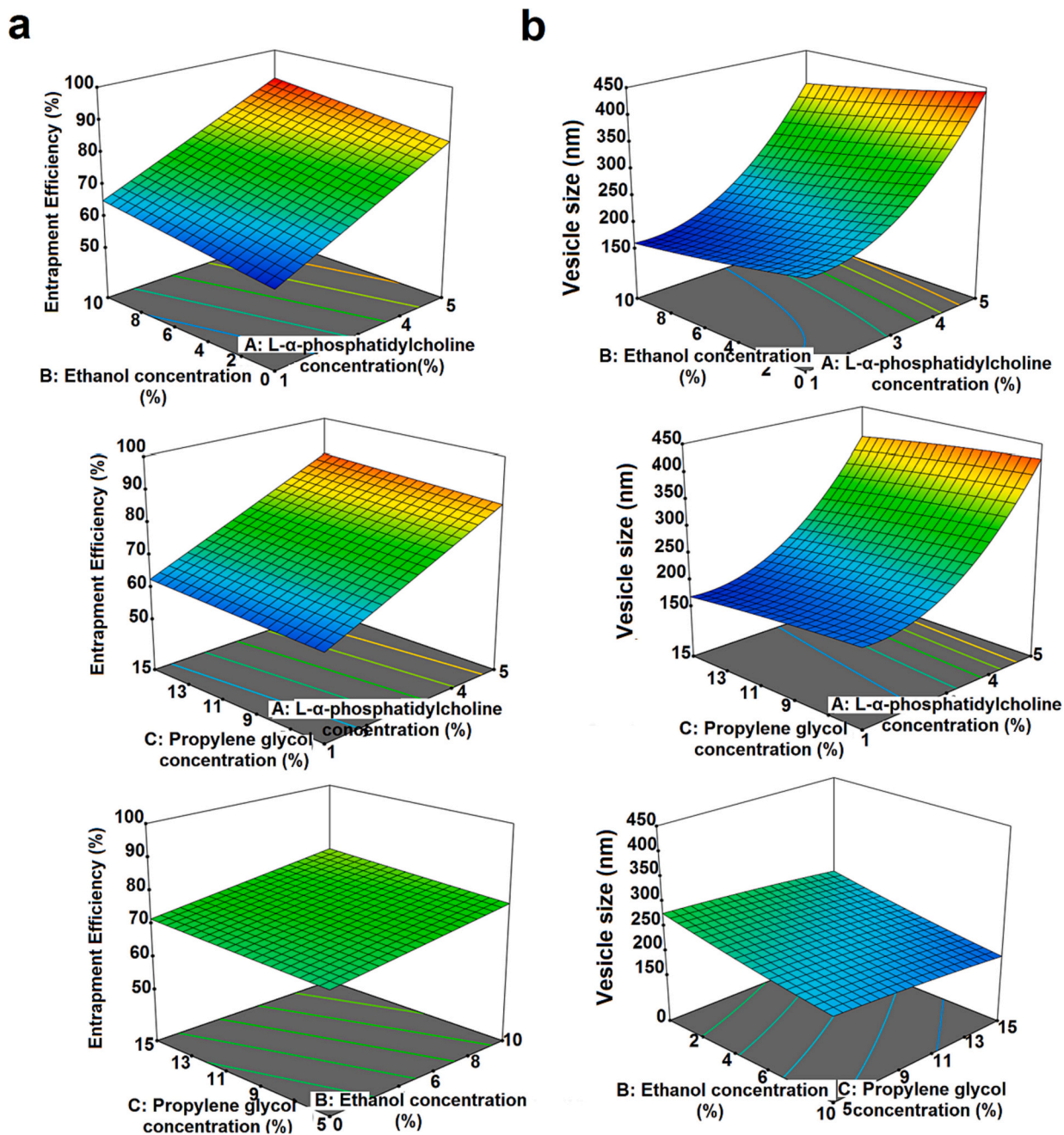


Fig. 2. 3D Response surface plot for the effect of L- α -phosphatidylcholine concentration, ethanol concentration and propylene glycol concentration on EE% (a) and particle size (b); 3D Response surface plot help users better understand the interaction between variables and their impact on each response.

α -phosphatidylcholine FTIR spectrum revealed peaks for the CH_2 stretching vibration at 2935 and 2862 cm^{-1} , the symmetrical $\text{C}=\text{O}$ stretching vibration at 1736 cm^{-1} , and the PO_4 antisymmetric stretching bands at 1243 cm^{-1} . The cholesterol FTIR spectrum revealed peaks for the OH stretching group at 3400 cm^{-1} , the CH_2 stretching vibration at 2940 cm^{-1} , the double bond $\text{C}=\text{C}$ at 1670 cm^{-1} and the asymmetric CH_2 stretching vibrations at 1459 cm^{-1} . The CDT FTIR spectrum revealed peaks for the CH stretching group at 2940 cm^{-1} , the carbonyl $\text{C}=\text{O}$ stretching at 1752 cm^{-1} , the aromatic $\text{C}-\text{N}$ stretching at 1350 cm^{-1} and the $\text{C}-\text{O}$ ether stretch at 1050 cm^{-1} . The FTIR spectra of the optimum CLEP formulation showed similar peaks of CDT, L- α -phosphatidylcholine and cholesterol.

3.4.3. Transmission electron microscopy (TEM)

The electron micrograph of the optimum CLEP formulation is shown in Fig. 4(a). The figure exhibited spherical vesicles that appeared as black dots and were evenly distributed and well separated from one another.

3.4.4. Zeta potential and size distribution

The PDI of the optimum CLEP formulation was determined to be 0.215 ± 0.07 , suggesting a homogeneous dispersion of vesicles, and the zeta potential was determined to be $-42.03 \pm 1.37\text{ mV}$, demonstrating its physical stability.

3.4.5. Stability study

The stability of the optimum CLEP formulation at 4°C , 25°C and

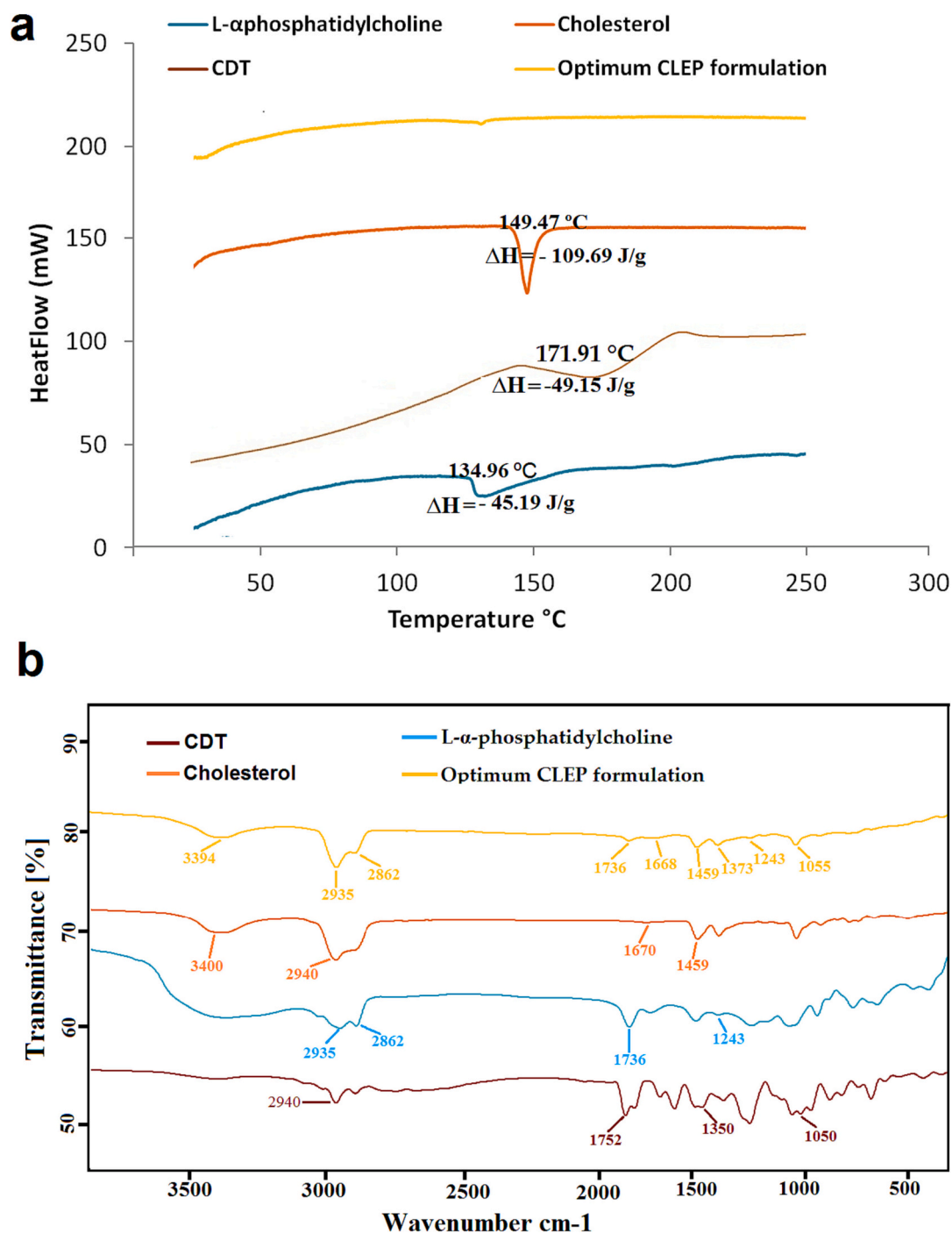


Fig. 3. a) Differential Scanning Calorimetry thermograms of optimum CLEP formulation which exhibited the disappearance of all peaks of CDT, L- α -phosphatidylcholine and cholesterol; (ΔH) enthalpy fusion; b) Fourier Transform Infrared (FTIR) spectra of optimum CLEP formulation which exhibited the appearance of all peaks of CDT, L- α -phosphatidylcholine and cholesterol.

40 °C is shown in Fig. 4(b). Using the ANOVA test, an insignificant decrease in EE% was observed for the CLEP formulation after being stored for three months at 4 °C, 25 °C, and 40 °C with a *p*-value (0 days vs 90 days) of 0.343, 0.553 and 0.398, respectively. Using the ANOVA test, an insignificant increase in particle size was observed for the CLEP formulation after being stored for three months at 4 °C, 25 °C, and 40 °C with a *p*-value (0 days vs 90 days) of 0.566, 0.473 and 0.296, respectively.

3.4.6. In vitro release study

The average cumulative CDT's released from the optimum CLEP

formulation in comparison to the free CDT is shown in Fig. 5(a). Using the Student *t*-test, we found that the optimum CLEP formulation significantly (*p*-value of <0.0001) increased the release of CDT relative to free CDT by a factor of 1.52 after 24 h.

3.4.7. Ex vivo skin permeation study

The mean cumulative CDT's permeated from the optimum CLEP formulation compared to the free CDT is shown in Fig. 5(b). Using the Student *t*-test, permeation of CDT from the free CDT dispersion (594.25 ± 11.92 $\mu\text{g}/\text{cm}^2$) was found to be significantly (*p*-value of <0.0001) lower than permeation of CDT from the optimum CLEP formulation

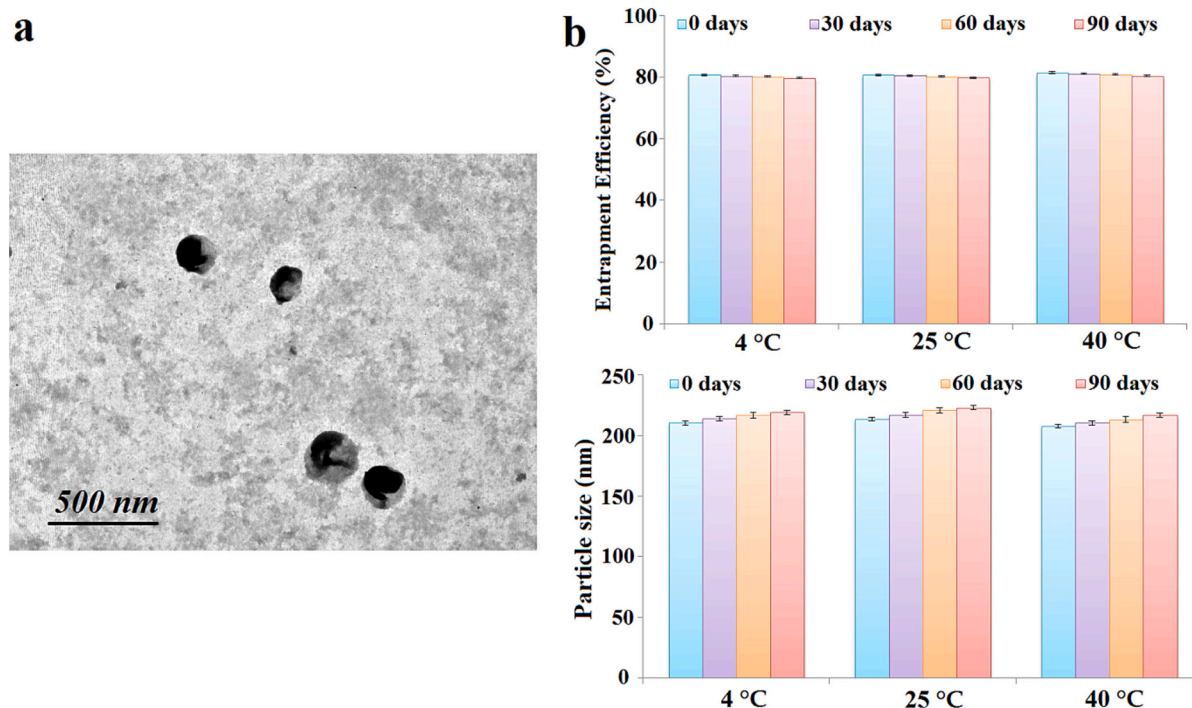


Fig. 4. a) Surface morphology of optimum CLEP formulation by TEM exhibited spherical vesicles that appeared as black dots; b) Effect of storage on the %EE and particle size of CLEP formulations at 4 °C, 25 °C and 40 °C.

($879.65 \pm 22.56 \mu\text{g}/\text{cm}^2$). Additionally, flux (J_{ss}) of optimum CLEP formulation ($33.75 \pm 0.94 \mu\text{g}/\text{cm}^2/\text{h}$) was significantly (p -value of <0.0001) higher than that of free CDT ($22.87 \pm 0.39 \mu\text{g}/\text{cm}^2/\text{h}$) with an enhancement ratio of 1.47 after 24 h.

3.5. In vivo evaluation of optimum CLEP formulation

3.5.1. Anti-ischemic stroke activity measurement

Diabetes and atherosclerosis were successfully induced, as shown by the control positive group's blood glucose, cholesterol, and TG levels being significantly (p -value of <0.0001) higher than those of the control negative group (Fig. 6a) by a ratio of 1.93, 6.11 and 1.65, respectively. Blood glucose levels were significantly (p -value of <0.0001) lower in the free CDT and optimum CLEP formulation groups compared to the control positive group (Fig. 6a) by 57.61% and 67.97%, respectively, showing their anti-diabetic activity. When compared to the free CDT group, blood glucose levels dropped significantly (p -value of 0.030) in the optimum CLEP formulation group, with a ratio of 1.18. Anti-atherosclerotic activities of free CDT and optimum CLEP formulation groups were demonstrated by a statistically significant (p -value of <0.0001) reduction in blood cholesterol and TG compared to the control positive group. In the free CDT group, the serum cholesterol and TG were decreased by 35.45% and 25.21%, respectively and in the optimum CLEP formulation group; they were decreased by 70.90% and 41.17%, respectively. When compared to the free CDT group, serum cholesterol and TG dropped significantly (p -value of <0.0001) in the optimum CLEP formulation group, with a ratio of 2 and 1.63, respectively. These findings suggest that both free CDT and the optimum CLEP formulation have anti-diabetic and anti-atherosclerotic effects; however, the optimum CLEP formulation group's effects were more potent than those of the free CDT group.

Compared to the control negative group, the control positive group's rats were shown to have significantly (p -value of <0.0001) higher flexion and spontaneous motor activities (Fig. 6b) by a ratio of 4 and 2.43, respectively, lower grip strength by a ratio of 2.5; and a longer time to locate the target quadrant by a ratio of 10.83. Based on these

behavioral deficits and neurological severity of the control positive group, it was determined that the ischemic stroke induction was successful. The anti-ischemic stroke activity of free CDT and the optimum CLEP formulation are shown in (Fig. 6b). Compared to the control positive group, the free CDT and the optimum CLEP formulation were shown to have significantly (p -value of <0.0001) lower flexion by 40% and 70%, respectively, lower spontaneous motor activity by 11.76% and 64.71%, respectively, lower time spent in the target quadrant by 78.46% and 92.31%, respectively, and higher grip strength by a ratio of 1.25 and 2.3, respectively. When compared to the free CDT group, flexion, spontaneous motor activity and the time spent in the target quadrant decreased significantly (p -value of <0.0001 , <0.0001 , 0.027, respectively) and grip strength increased significantly (p -value of <0.0001) in the optimum CLEP formulation group, with a ratio of 1.75, 5.5, 1.17 and 1.84, respectively. These findings suggest that both free CDT and the optimum CLEP formulation have anti-ischemic stroke activity; however, the optimum CLEP formulation group's effects were more potent than those of the free CDT group.

To confirm the induction of ischemic stroke in rats, we compared the histopathology of the control positive group, as shown in Fig. 7, to that of the control negative group. Photomicrographs from the control positive group revealed abnormalities in the histopathological structure of the brain tissue compared to the control negative group. These abnormalities included congestion of minute blood capillaries (black arrow) with perivascular edoema (red arrow), the presence of dead shrunken neurons (blue arrow), and the pyknotic nuclei of some neurons (arrow head). Fig. 7 also demonstrates the anti-ischemic stroke activity of both free CDT and the optimum CLEP formulation, as seen by the reduction in edoema (arrow head), dead shrunken neurons, and vascular congestion. However, the optimum CLEP formulation group was found to have higher anti-ischemic stroke activity with normal structured neurons (yellow arrows) than the free CDT group.

3.5.2. Toxicity studies

There was statistically insignificant (p -value of 0.542) difference in body weight or behavior between the optimum CLEP formulation group

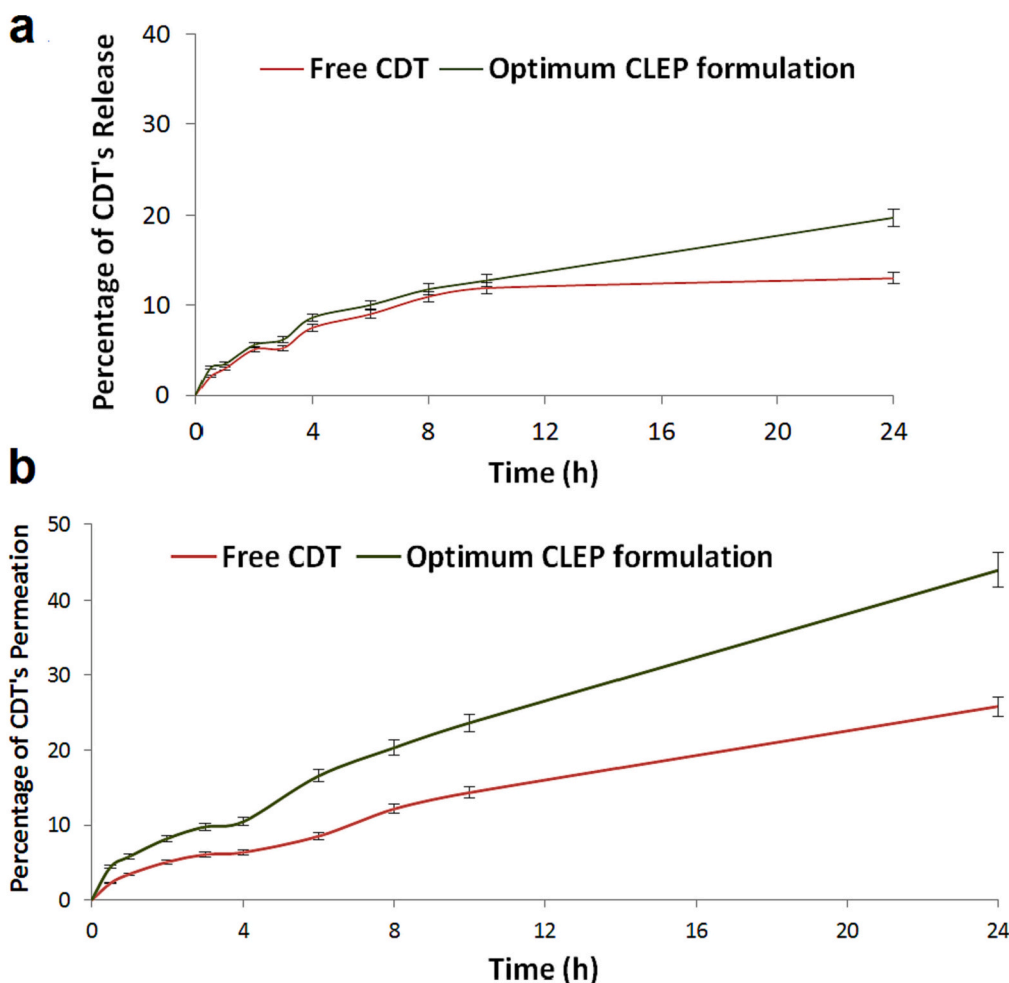


Fig. 5. a) The percentage of CDT release from the optimum CLEP formulation in comparison to free CDT, in phosphate buffer (pH 6.8, mean \pm S.D., $n = 3$); b) the percentage of CDT permeation from the optimum CLEP formulation in comparison to free CDT in phosphate buffer (pH 6.8, mean \pm S.D., $n = 3$).

and the control negative group at the end of the trial. No skin, sleep, salivation, or diarrhoea side effects were recorded after daily nasal administration of the optimum CLEP formulation throughout the studies. Fig. 8 demonstrates no toxicity issues were found after the nasal administration of the optimum CLEP formulation because the rats in the optimum CLEP formulation group exhibited non-significant (p -values are shown in Fig. 8) changes in haematological and biochemical parameters compared with the control negative group.

4. Discussion

Although various preventive therapies for diabetes associated stroke have been developed, their clinical implementation has been hindered by challenges such as insolubility, short half-life, limited permeability across the blood-brain barrier, and poor accumulation on the ischemic tissue (Saxena et al., 2015; Campos-Martorell et al., 2016; Bruch et al., 2019; Bernardo-Castro et al., 2021). Considering this, nanotechnology has potential benefits for developing new stroke therapeutics. Liposomes are a type of nanovesicular drug delivery system that facilitate the transportation of medications across the blood-brain barrier (BBB), hence enhancing their accumulation within the brain (Campos-Martorell et al., 2016; Fukuta et al., 2017; Bruch et al., 2019; Bernardo-Castro et al., 2021). Campos-Martorell et al. develop a new liposomal delivery system to increase BBB permeability and simvastatin's accumulation in the ischemic brain (Campos-Martorell et al., 2016). A formulation of neuroprotectant-loaded liposome conjugated with T7 peptide and stroke homing peptide was developed by Yue et al. for improving the blood-

brain barrier permeability and brain targeting (Zhao et al., 2016). The study conducted by Fukuta et al. provided evidence supporting the effectiveness of a combined treatment approach involving liposomal neuroprotectants and tissue plasminogen activator in the management of ischemic stroke (Fukuta et al., 2017). Despite their effectiveness, liposomes have a number of drawbacks, including drug leakage, poor stability and poor permeability (Alavi et al., 2017). This study aimed to develop liposomes containing ethanol and propylene glycol formulation as a potential drug delivery carrier for diabetes-associated stroke treatment.

Candesartan has been used to prevent stroke, but it has poor absorption, solubility and efficacy. Liposomes containing ethanol and propylene glycol formulations are liposomal nano-vesicles made of penetration enhancers such as ethanol and propylene glycol (Zhang et al., 2012a, 2012b; Abdulbaqi et al., 2016; Salem et al., 2021). L- α phosphatidylcholine are the building blocks of vesicles (Abdulbaqi et al., 2016; Salem et al., 2021). Cholesterol was added because it improves membrane integrity and drug entrapment by filling in the gaps between the poorly packed lipid species in vesicular membranes (Abdulbaqi et al., 2016; Salem et al., 2021). Touitou et al. presented a novel vesicular system that has a high concentration of ethanol (Touitou et al., 2000). Ethanol is a powerful penetration enhancer because it softens the vesicles, allowing them to penetrate deeper layers of skin, and makes them smaller and, therefore, increasing their surface area and absorption (Touitou et al., 2000; Abdulbaqi et al., 2016). However, the vesicle membranes become more permeable and the drug entrapment drops when ethanol concentrations are high (Zhang et al., 2012a, 2012b;

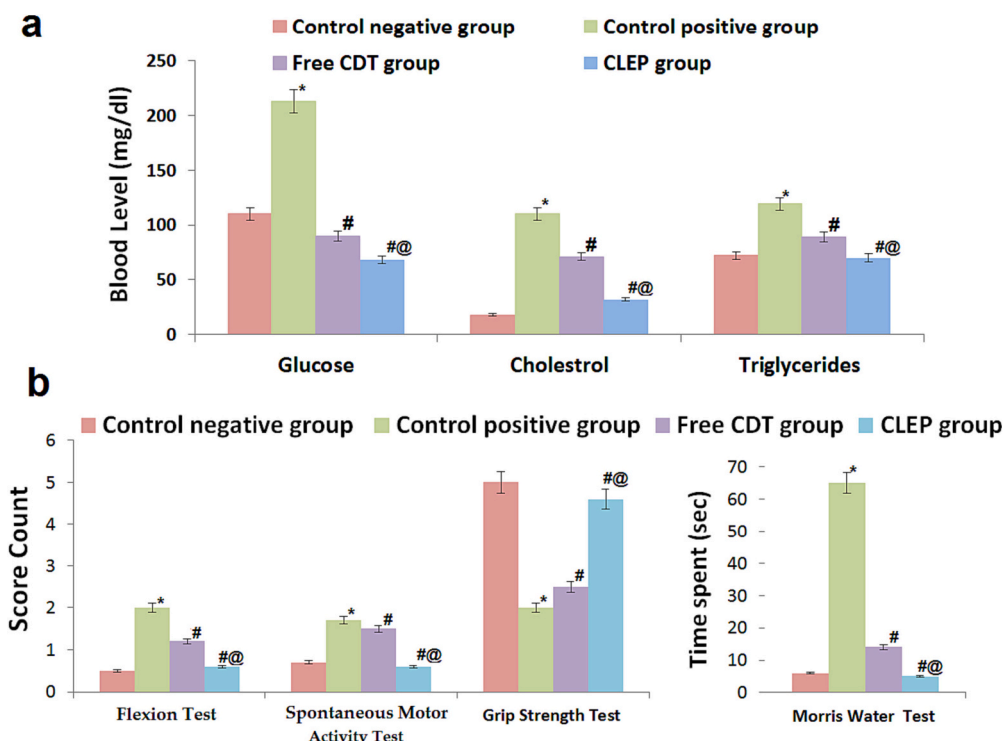


Fig. 6. a) Serum glucose, cholesterol and triglycerides levels; b) Neurological behavioral activities in rats of all treated and untreated groups; Significance: * p-value <0.05 versus control negative group, # p-value <0.05 versus control positive group, @ p-value <0.05 versus free CDT group. CDT: candesartan, CLEP: candesartan loaded liposomes containing ethanol and propylene glycol.

Abdulbaqi et al., 2016). Salem et al. studied propylene glycol as a component of lipid vesicles and evaluated propylene glycol-liposomes as carriers for the topical administration of Raloxifene (Salem et al., 2021). Propylene glycol is a widely used penetration enhancer which makes the drug permeate into the skin more easily (Zhang et al., 2012a, 2012b; Salem et al., 2021). It has been found that propylene glycol can prevent vesicle aggregates in formulations (Manconi et al., 2009). As it is more viscous and hygroscopic than ethanol, propylene glycol may increase vesicle affinity to molecules in the water-based dermis layer, so slowing the vesicles' transit through the skin and increasing their concentration in the deep skin (Shen et al., 2014). When ethanol and propylene glycol combine, they increase the skin' fluidity (Zhang et al., 2012a, 2012b; Abdulbaqi et al., 2016). Previous research assessed the safety and cytotoxicity of ethanol and propylene glycol (Holmberg and Malmfors, 1974; Lachenmeier, 2008; HAMZELOO et al., 2014; Ilieva et al., 2021). It has been established that ethanol and propylene glycol are safe (Holmberg and Malmfors, 1974). Based on the MTT and AST assays, the cytotoxic and microbicidal effects of ethanol and propylene glycol were studied by Ilieva et al., and the results indicated that they are likely safe to use (Ilieva et al., 2021). Therefore, our study used design expert software to analyze the impacts of different ethanol, L- α -phosphatidylcholine, and propylene glycol concentrations as independent variables. Independent variable concentration ranges were determined through literature reviews and preliminary experiments.

The CLEP formulation was optimized by employing a Box-Behnken design using the ANOVA test, adjusted R^2 , predicted R^2 and adequate precision. The optimum model should have a high values of adjusted R^2 and predicted R^2 with a discrepancy of <0.2 (Abdelbary and AbouGhaly, 2015; Awan et al., 2022). Adequate precision is a signal-to-noise ratio that should be >4, and then the model's ability to discriminate is good enough (Abdelbary and AbouGhaly, 2015; Awan et al., 2022). Results from both EE% and particle size suggested that the quadratic model was the most appropriate fit. Box-Cox and Residual vs. expected response graphs are produced by Design Expert® software to further assess the

quality of the quadratic model fit (Abdelbary and AbouGhaly, 2015; Awan et al., 2022). A Box-Cox plot can be used to help choose the best power transformation for each response data according to the value of lambda (λ). No transformation is needed if $\lambda \geq 1$. Residual versus predicted plot can be used to examine the distribution of residuals. Presence of a random scatter of residuals across the graph indicated no transformation is required for EE% and particle size data.

To understand the interaction between independent variables and the effect of each variable and interpret the model, the software generated 3D charts and polynomial equations in terms of coded values. When the concentration of L- α -phosphatidylcholine was raised, the EE% was significantly (p-value of <0.0001) increased because strong coherent layers form around individual vesicles, and shell-like structures are built around the medication, potentially reducing its rate of leakage. Additionally, the CDT's lipophilic properties and limited water solubility blame for its high EE%. When the concentration of L- α -phosphatidylcholine was raised, the particle size was significantly (p-value of <0.0001) increased because the accompanying increase in viscous phase and mass transfer resistance causes bigger nanoparticles to be formed. Similar results were noted for raloxifene propylene glycol-liposomes upon increasing phospholipid from 1% to 3% (Salem et al., 2021). When the concentrations of ethanol and propylene glycol were raised, the EE% was significantly (p-value of <0.0001) increased because higher concentrations of ethanol and propylene glycol enhance drug solubility, leading to more entrapment and more even drug distribution within the vesicle. When the concentrations of ethanol and propylene glycol were raised, the particle size was significantly (p-value of <0.0001) decreased because vesicles' thickness was decreased and their net charge was changed when ethanol and propylene glycol concentrations were increased. Furthermore, ethanol and propylene glycol have a fluidizing impact on L- α -phosphatidylcholine bilayers, leading to compact, soft, deformable vesicles. In consistency with Li et al., they found that the addition of propylene glycol (0–30%) and ethanol (0–30%) enhanced transdermal entrapment and permeation of

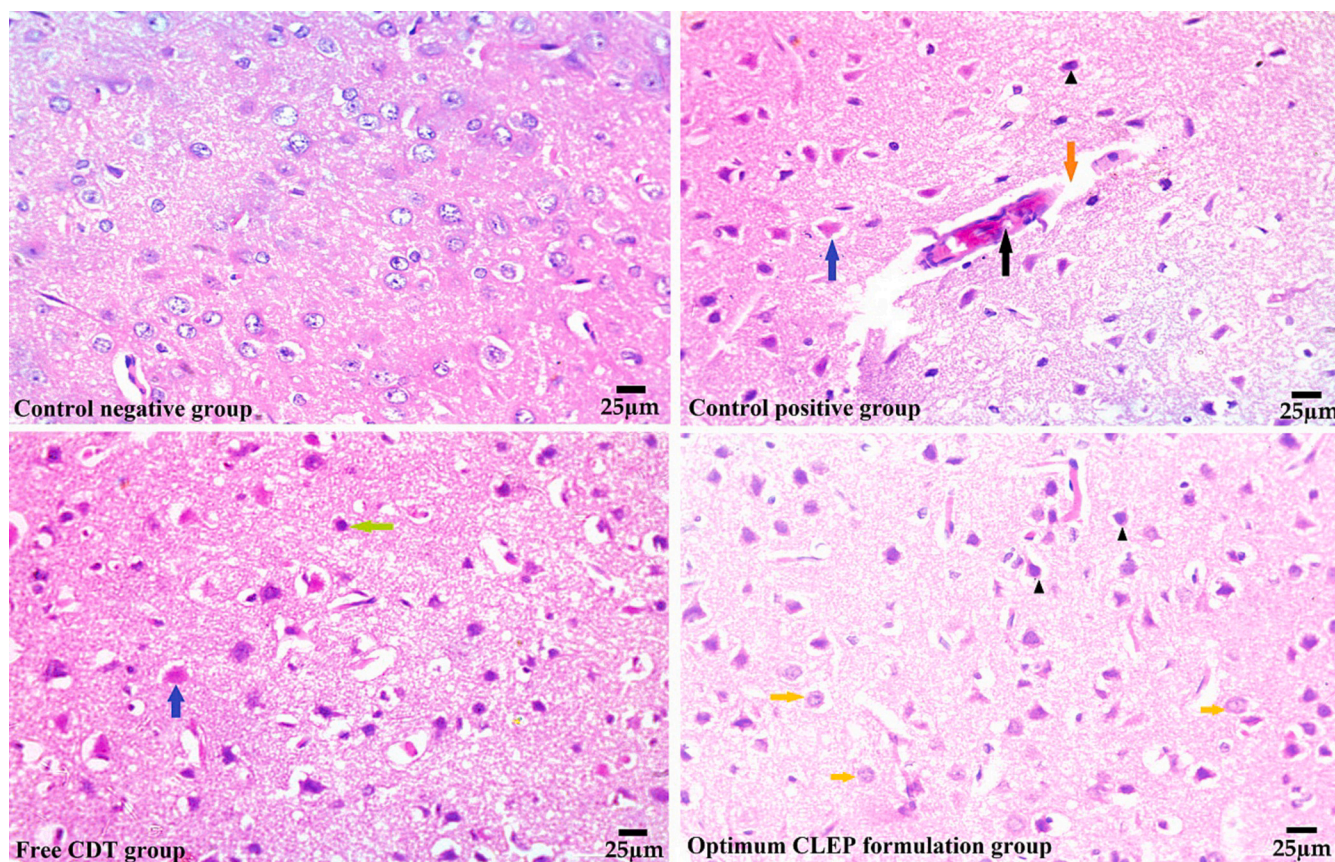


Fig. 7. Histopathology images of brain tissue in normal rats and rats of all treated and untreated groups. Blue arrow: dead shrunken neurons, red arrow: perivascular edema, green arrow and arrow head: pyknotic nuclei of some neurons, and yellow arrows: normal structured neurons. CDT: candesartan, CLEP: candesartan loaded liposomes containing ethanol and propylene glycol. (For interpretation of the references to colour in this figure legend, the reader is referred to the web version of this article.)

tacrolimus (Li et al., 2012).

A desirability index was utilized in conjunction with numerical optimization to determine the optimum formulation, which was then produced and validated. Since there was no significant discrepancy between the observed and predicted values, the results validate the optimization procedure. DSC is a thermotropic technique utilized to evaluate the crystallinity and thermal behavior of the drug in the developed systems and to annotate its potential interactions with other components (Gamal et al., 2021). The enthalpy fusion is the amount of energy absorbed by a solid during its melting process. Distinct endothermic peaks of separate components disappeared in the DSC thermograms of optimum formulation, which may be due to the existence of the CDT in an amorphous state and its imprisonment in the lipid bilayer of the CLEP formulation. This discussion was corroborated by FT-IR spectra, which is used to determine any incompatibility between the components of the optimum CLEP formulation and confirm the results of DSC (Xu et al., 2022). FTIR spectra showed that the optimum CLEP formulation had the same spectra as CDT, cholesterol, and L- α -phosphatidylcholine. This suggested that the components of the formulation were compatible, and that CDT had been successfully incorporated into the vesicles without any chemical interaction.

To assess the homogeneity of the optimum CLEP formulation, particle size distribution in term of PDI was determined (El-Ela et al., 2022). Low PDI of the optimum CLEP formulation showed that there was a monodisperse and uniform distribution of vesicles. Zeta potential is a vital indicator of the physical stability of the produced dispersions (El-Ela et al., 2022). The stability of the optimum CLEP formulation was demonstrated by its negative zeta potential due to the presence of L- α -phosphatidylcholine. Additionally, ethanol increases the stability of

the CLEP and inhibits the vesicles from clustering due to electrostatic repulsion. Propylene glycol increases the stability of the CLEP by increasing the viscosity of vesicular formulations. The stability investigation of the optimum CLEP formulation corroborated these findings by showing that the EE% and particle size of the optimum CLEP formulation changed insignificantly after being stored for three months at 4 °C, 25 °C, and 40 °C. Previous studies have shown that combining ethanol and propylene glycol can greatly improve the stability of terbinafine-loaded binary ethosomes (Zhang et al., 2012a, 2012b). Transmission electron microscopy provided representative micrographs of the optimum CLEP formulation and verified the presence of nano-sized vesicles that were not aggregated.

A study of CDT's equilibrium solubility was conducted to ascertain how much dissolution media would be required to reach the sink condition. Dissolution was achieved in 50 mL of phosphate-buffered (pH 6.8) with 0.1% (w/w) Tween 80, which is greater than the saturation solubility of CDT. Based on the in vitro drug release profile, the optimum CLEP formulation enhanced the CDT's release due to its solubilizing effect, resulting in improved the aqueous solubility of CDT, which in turn improved its oral bioavailability. These results confirmed that vesicular encapsulation of CDT altered its crystalline structure into a soluble amorphous form, resulting in CDT's release. These results are consistent with those found in a different paper by Sezgin-Bayindir et al., who looked at how adding nanoparticles such as mixed niosomes to candesartan increased its solubility in water (Sezgin-Bayindir et al., 2015). When ethanol and propylene glycol combine, they make the lipid bilayer more malleable and fluid and boost vesicle deformability; therefore, the optimum CLEP formulation exhibited better permeability. These findings are in accord with another report by Shen et al., who

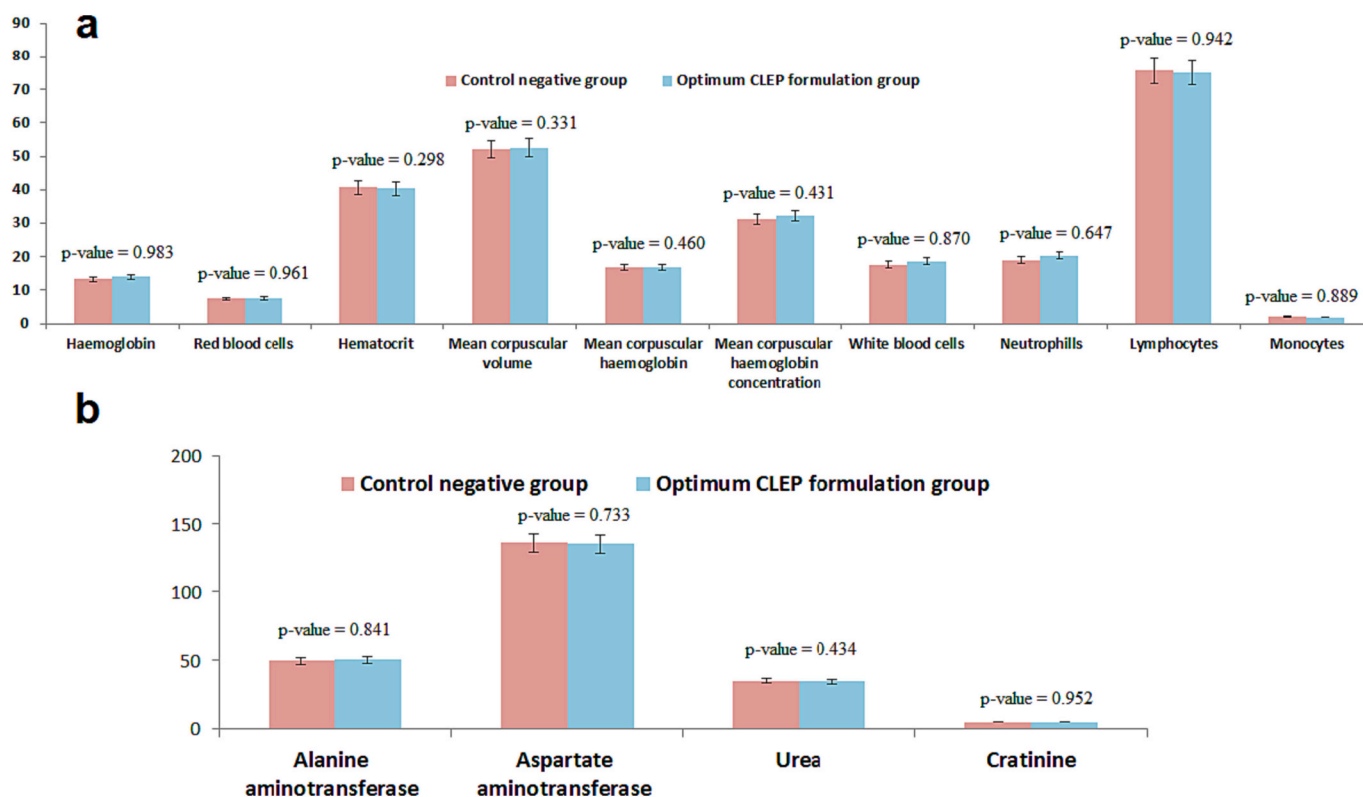


Fig. 8. Haematological (a) and biochemical (b) parameters of optimum CLEP group compared to control negative group. Significance: # p-value <0.05 versus control negative group.

improved the skin deposition of apigenin by adding ethanol and propylene glycol to liposomes (Shen et al., 2014).

Diabetes mellitus increases the risk and severity of stroke because hyperglycemia is associated with malfunction of endothelial cells, thickening of the capillary basal membrane and increased arterial stiffness (Policardo et al., 2015; Tuttolomondo et al., 2015; Mosenzon et al., 2023). Coexisting atherosclerosis has been proven to have better predictive value for stroke due to its capacity to drive inflammatory cell infiltration and phagocytosis, as well as plaques calcification following endothelial damage (Wouters et al., 2005; Hadaegh et al., 2012; Banerjee and Chimowitz, 2017; Li et al., 2018; Lian et al., 2018). Accordingly, we hastened the progression of an experimental model of ischemic stroke in rats by developing diabetes and atherosclerosis in them by feeding them sugar in addition to a high-fat diet for a period of 12 weeks (Lian et al., 2018; Pérez-Corredor et al., 2022). Pérez-Corredor et al. investigated the effect of a high sugar diet on the brain following cerebral ischemia in rats and found that neuronal loss, inflammation, and plasticity impairment after cerebral ischemia were all exacerbated (Pérez-Corredor et al., 2022). Lian et al.'s study showed that a high-fat diet, administered to rats for 12 weeks, successfully promoted the onset of atherosclerosis (Lian et al., 2018).

Monitoring serum glucose, TG, and cholesterol levels confirmed the successful production of diabetes and atherosclerosis (Akbarzadeh et al., 2007; Ekeanyanwu and Njoku, 2014; Kumar et al., 2017). Blood glucose levels were significantly higher in the control positive group in contrast to normal rats, demonstrating the successful establishment of experimental diabetes in rats. Consuming an excessive quantity of sugar resulted in a caloric excess, which in turn caused obesity accompanied by dyslipidemia, weight gain, glucose intolerance, and fatty liver. The findings of our study were consistent with those reported by (Pérez-Corredor et al., 2022). Blood cholesterol and triglycerides levels were significantly higher in the control positive group in contrast to normal rats, demonstrating the successful establishment of experimental

atherosclerosis in rats. Excessive fat consumption resulted in lipid buildup in the arteries, which encouraged inflammatory cell infiltration and phagocytosis, as well as plaque calcification. Our results agreed with those found by (Lian et al., 2018).

Ischemic stroke was induced by occluding the middle cerebral arteries with an intraluminal suture. Because of this occlusion, brain oxygen levels drop, which in turn triggers a cascade of negative physiological responses including oxidative stress, inflammation, and apoptosis (Ashafaq et al., 2021). Stroke was successfully induced in rats as evidenced by histopathological evaluation, which revealed the existence of congestive blood capillaries, edoema, and dead, shrunken neurons in control positive mice. Furthermore, the discovery of severe behavior and memory abnormalities in control positive rats verified the successful creation of the rat experimental stroke model. Compared to the normal rats, the control positive group showed significantly higher flexion and spontaneous motor activities, lower grip strength, and a longer time to locate the target quadrant. Our findings were in agreement with the outcomes reported by Ashafaq et al., who examined the impact of resveratrol nanoparticles on oxidative stress, memory impairment, and behavioral activities in rats following ischemic stroke (Ashafaq et al., 2021).

Among treatment groups, both free CDT and optimum CLEP formulation significantly (p -value of <0.0001) attenuated the hyperglycemia and neurological consequences of control positive group, showing the therapeutic potential. CDT is a potential angiotensin II receptor antagonist that reduces cerebrovascular vasoconstriction, oxidative damage, apoptosis and inflammation. Our results were consistent with those of Ding et al. and Zhou et al., who discovered that candesartan could prevent brain ischemia (Zhou et al., 2006; Ding et al., 2022). Additionally, Hyperglycemia can also be reduced because of CDT's ability to reduce insulin resistance and glucose intolerance. Nakao et al. demonstrated that candesartan medication decreased the occurrence of new-onset diabetes in obese patients, and our results

corroborated those findings (Nakao et al., 2010). The optimum CLEP formulation group's effects were more potent than those of the free CDT group because the optimum CLEP formulation had a solubilizing effect, resulting in improved drug release and the aqueous solubility of CDT. The synergistic effect of ethanol/propylene glycol and smaller the size of the CLEP nanoparticles increased permeation and transport across blood brain barrier of CDT. Additionally, the nasal cavity's large surface area and intricate system of blood arteries expedite the drug's entry into the systemic circulation, skipping first-pass metabolism along the way. In the previous study conducted by Ashafaq et al., they found that resveratrol nanoparticles improved memory impairment and motor activities in rats following ischemic stroke (Ashafaq et al., 2021). Resveratrol nanoparticles at a dose of 500 mg/Kg significantly reduced flexion by 64%, reduced spontaneous motor activities by 60%, improved grip strength with a ratio of 2, and reduced time to locate the target quadrant by 57% when compared with the positive control (MCAO) rats. Application of the nasal CLEP formulation at a dose of 1 mg/Kg significantly reduced flexion by 70%, reduced spontaneous motor activities by 64.71%, improved grip strength with a ratio of 2.3, and reduced time to locate the target quadrant by 92.31% when compared with the positive control rats. Therefore, the nasal administration of CLEP drops could be a potential diabetes-associated stroke treatment.

To determine the safety of an optimum CLEP formulation, toxicological evaluations such as body weight, haematological, renal, and liver functions were performed on experimental rats (Ekeanyanwu and Njoku, 2014; Porwal et al., 2017). There was no significant (p -value of 0.542) difference in weight gain between the optimum CLEP formulation group and the control negative group of rats, suggesting that the nasal administration of the formulation had no negative influence on the animals' growth and development. The animals' erythropoiesis and immune systems did not change after receiving the optimum CLEP formulation via the nasal route, since none of the haematological data were significantly different from the control negative group. Urea, creatinine, alanine aminotransferase, and aspartate aminotransferase levels did not significantly change, suggesting that the optimum CLEP formulation is not harmful to kidney and liver function.

There are some limitations to our research, such as the method of diabetes that was induced, the fact that only male rats were included, and the length of the treatment. Streptozotocin is the most widely utilized diabetogenic drug for induction of hyperglycemia (Ghasemi and Jeddi, 2023). We decided to add refined sugar instead of streptozotocin injection because induction of hyperglycemia in rats without prior diabetes has the worst outcomes of both acute and chronic hyperglycemia (Zsuga et al., 2012). Consequently, the duration of the induction phase was prolonged. Stroke risk and prognosis in diabetics have been shown to vary by gender in clinical studies (Policardo et al., 2015). We excluded the use of female rats because the outcomes of hyperglycemia induction were less severe when the female gender was included (Vannucci et al., 2001). The experimental groups, namely the free CDT group and CLEP group, received a treatment period of 10 days before the induction of ischemic stroke. This short treatment period influenced the observed outcomes in these groups, as compared to the positive control group. Histopathological analysis of the experimental groups revealed a decrease, not a complete eradication, of dead shrunken neurons and vascular congestion. All these limitations will be applied in the future, and our next publication will take them into account.

Animal models have consistently proven to be the most effective alternative method for testing theories prior to doing human studies (Ghasemi and Jeddi, 2023). They serve as a fundamental component of preclinical drug development. The data derived from our *in vivo* studies exhibit a high level of significance. Our study sought to report that the design of CLEP formulation has the potential to radically alter the landscape for stroke management, from the enhancement of existing therapies to new ones aiming to prevent and even restore the ischemic brain, ultimately leading to better care and clinical advancement for patients. In our study, it was discovered that the development of CLEP

formulation resulted in enhanced delivery, release, permeation, and efficacy of candesartan in an experimental rat model of stroke and diabetes, compared with that of free candesartan. This potential development holds significant promise for patients receiving candesartan as a treatment for stroke associated diabetes. It has the potential to provide a reduction in dosage, hence minimizing the likelihood of experiencing adverse effects. Additionally, the data given in this article suggests that the advantages of utilizing CLEP formulation extend beyond individuals with diabetes-associated stroke to include those with hypertension as well. Our study provided complete interpretations about the anti-diabetes associated-stroke effectiveness and toxicity of candesartan *in vivo*. However, well-planned clinical trials are still needed to be conducted to get approval for human use.

A highlighted area of our future research is the potential expansion of CLEP formulation through the incorporation of specialized ligands onto its surface. This modification aims to selectively target the transferrin receptor in the brain, with the objective of enhancing the specificity of candesartan and augmenting its concentration within the brain. An *in vitro* and *in vivo* comparative study will be conducted to evaluate the effectiveness and targeting capabilities of conventional CLEP formulation and transferrin-modified CLEP formulation for the treatment of diabetes associated stroke. Additionally, the evaluation of bioavailability and other pharmacokinetic parameters for both the conventional CLEP formulation and the transferrin-modified CLEP formulation will be conducted by analyzing the profile of plasma levels over time.

5. Conclusion

The purpose of this study was to develop a nasal CLEP formulation drops as a potential diabetes-associated stroke treatment. When compared to free CDT, the CLEP formulation showed smaller vesicles, increased drug release, and enhanced nasal permeation. The CLEP formulation showed a greater *in vivo* reduction of edoema, dead shrunken neurons, and vascular congestion induced by occlusion of the common carotid and middle cerebral arteries in comparison to control positive rats. In conclusion, the present study demonstrates that nasal CLEP treatment improved neurobehavioral outcome and reduced the infarction. Therefore, the nasal administration of CLEP drops could be a potential diabetes-associated stroke treatment.

Institutional review board statement

The ethics committee at Beni-Suef University in Egypt gave their stamp of approval (BSU-IACUC: 022–414).

Funding

The "Prince Sattam Bin Abdulaziz University Project number (PSAU/2023/R/1445) and King Saud University Researchers Supporting Project number (RSP2023R211), Riyadh, Saudi Arabia," provided funding for this study.

CRediT authorship contribution statement

Dina M. Mahmoud: Investigation, Methodology, Writing – original draft. **Mohammed R.A. Ali:** Data curation, Methodology, Software, Writing – original draft. **Basmah Nasser Aldosari:** Conceptualization, Funding acquisition, Resources, Validation, Writing – review & editing. **Randa Mohammed Zaki:** Funding acquisition, Resources, Software, Validation, Writing – original draft. **Obaid Afzal:** Funding acquisition, Resources, Software, Validation, Writing – review & editing. **Alaa S. Tulbah:** Formal analysis, Resources, Software, Writing – review & editing. **Demiana M. Naguib:** Formal analysis, Investigation, Methodology, Visualization. **Mohamed I. Zanaty:** Formal analysis, Investigation, Methodology, Visualization. **Mary Eskander Attia:** Formal analysis, Methodology, Writing – original draft. **Fatma I. Abo El-El:**

Conceptualization, Methodology, Writing – original draft. **Amr Gamal Fouad:** Conceptualization, Methodology, Writing – original draft.

Declaration of competing interest

The authors declare the following financial interests/personal relationships which may be considered as potential competing interests:

Basmah nasser reports financial support was provided by King Saud University. Randa Zaki reports a relationship with Prince Sattam bin Abdulaziz University that includes: employment and funding grants.

Data availability

Data will be made available on request.

Acknowledgements

This study was supported via funding from Prince Sattam Bin Abdulaziz University Project number (PSAU/2023/R/1445) and a grant from “Researchers Supporting Project number (RSP2023R211), King Saud University, Riyadh, Saudi Arabia

References

- Abdelbary, A.A., AbouGhaly, M.H., 2015. Design and optimization of topical methotrexate loaded niosomes for enhanced management of psoriasis: application of Box–Behnken design, in-vitro evaluation and in-vivo skin deposition study. *Int. J. Pharm.* 485 (1–2), 235–243. <https://doi.org/10.1016/j.ijpharm.2015.03.020>.
- Abdulbaqi, I.M., Darwis, Y., Khan, N.A.K., Abou Assi, R., Khan, A.A., 2016. Ethosomal nanocarriers: the impact of constituents and formulation techniques on ethosomal properties, in vivo studies, and clinical trials. *Int. J. Nanomedicine* 11, 2279. <https://doi.org/10.2147/IJN.S105016>.
- Akbarzadeh, A., Norouzi, D., Mehrabi, M., Jamshidi, S., Farhangi, A., Verdi, A.A., Rad, B.L., 2007. Induction of diabetes by streptozotocin in rats. *Indian J. Clin. Biochem.* 22, 60–64. <https://doi.org/10.1007/BF02913315>.
- Alavi, M., Karimi, N., Safaei, M., 2017. Application of various types of liposomes in drug delivery systems. *Adv. Pharm. Bull.* 7 (1), 3. <https://doi.org/10.15171/apb.2017.002>.
- Aly, U.F., Sarhan, H.A.-M., Ali, T.F., Sharkawy, H.A.E.-B., 2020. Applying different techniques to improve the bioavailability of candesartan cilexetil antihypertensive drug. *Drug Des. Devel. Ther.* 14, 1851–1865. <https://doi.org/10.2147/DDDT.S248511>.
- Ashafaq, M., Alam, M.I., Khan, A., Islam, F., Khuwaja, G., Hussain, S., Alhazmi, H.A., 2021. Nanoparticles of resveratrol attenuates oxidative stress and inflammation after ischemic stroke in rats. *Int. Immunopharmacol.* 94, 107494. <https://doi.org/10.1016/j.intimp.2021.107494>.
- Awan, Z.A., AlGhamdi, S.A., Alhakamy, N.A., Okbazghi, S.Z., Alfaleh, M.A., Badr-Eldin, S.M., Zakai, S.A., 2022. Optimized 2-methoxyestradiol invasomes fortified with apamin: a promising approach for suppression of A549 lung cancer cells. *Drug Deliv.* 29 (1), 1536–1548. <https://doi.org/10.1080/10717544.2022.2072412>.
- Banerjee, C., Chimowitz, M.I., 2017. Stroke caused by atherosclerosis of the major intracranial arteries. *Circ. Res.* 120 (3), 502–513. <https://doi.org/10.1161/CIRCRESAHA.116.308441>.
- Bernardo-Castro, S., Albino, I., Barrera-Sandoval, Á.M., Tomatis, F., Sousa, J.A., Martins, E., Sargento-Freitas, J., 2021. Therapeutic nanoparticles for the different phases of ischemic stroke. *Life* 11 (6), 482. <https://doi.org/10.3390/life11060482>.
- Bruch, G.E., Fernandes, L.F., Bassi, B.L., Alves, M.T.R., Pereira, I.O., Frézar, F., Massensini, A.R., 2019. Liposomes for drug delivery in stroke. *Brain Res. Bull.* 152, 246–256. <https://doi.org/10.1016/j.brainresbull.2019.07.015>.
- Campos-Martorell, M., Cano-Sarabia, M., Simats, A., Hernández-Guillamon, M., Rosell, A., Maspoch, D., Montaner, J., 2016. Charge effect of a liposomal delivery system encapsulating simvastatin to treat experimental ischemic stroke in rats. *Int. J. Nanomedicine* 11, 3035–3048. <https://doi.org/10.2147/IJN.S107292>.
- Cunha, S., Amaral, M., Lobo, J.S., Silva, A., 2017. Lipid nanoparticles for nasal/intranasal drug delivery. *Crit. Rev. Ther. Drug Carrier Syst.* 34 (3), 257–282. <https://doi.org/10.1615/CritRevTherDrugCarrierSyst.2017018693>.
- Ding, Y., Lang, Y., Zhang, H., Li, Y., Liu, X., Li, M., 2022. Candesartan reduces neuronal apoptosis caused by ischemic stroke via regulating the FFAR1/ITGA4 pathway. *Mediat. Inflamm.* <https://doi.org/10.1155/2022/2356507>.
- Dudhipala, N., Veerabrahma, K., 2016. Candesartan cilexetil loaded solid lipid nanoparticles for oral delivery: characterization, pharmacokinetic and pharmacodynamic evaluation. *Drug Deliv.* 23 (2), 395–404. <https://doi.org/10.3109/10717544.2014.914986>.
- Ekeanyanwu, R.C., Njoku, O.U., 2014. Acute and subacute oral toxicity study on the flavonoid rich fraction of *Monodora tenuifolia* seed in albino rats. *Asian Pac. J. Trop. Biomed.* 4 (3), 194–202. [https://doi.org/10.1016/S2221-1691\(14\)60231-8](https://doi.org/10.1016/S2221-1691(14)60231-8).
- El-Ela, F.I.A., Gamal, A., Elbanna, H.A., ElBanna, A.H., Salem, H.F., Tulbah, A.S., 2022. In vitro and in vivo evaluation of the effectiveness and safety of amygdalin as a cancer therapy. *Pharmaceutics* 15 (11), 1306. <https://doi.org/10.3390/ph15111306>.
- Fasiolo, L.T., Manniello, M.D., Tratta, E., Buttini, F., Rossi, A., Sonvico, F., Colombo, G., 2018. Opportunity and challenges of nasal powders: Drug formulation and delivery. *Eur. J. Pharm. Sci.* 113, 2–17. <https://doi.org/10.1016/j.ejps.2017.09.027>.
- Fukuta, T., Asai, T., Yanagida, Y., Namba, M., Koide, H., Shimizu, K., Oku, N., 2017. Combination therapy with liposomal neuroprotectants and tissue plasminogen activator for treatment of ischemic stroke. *FASEB J.* 31 (5), 1879–1890. <https://doi.org/10.1096/fj.201601209R>.
- Gamal, F.A., Kharshoum, R.M., Sayed, O.M., El-Ela, F.I.A., Salem, H.F., 2020. Control of basal cell carcinoma via positively charged ethosomes of Vismodegib: in vitro and in vivo studies. *J. Drug Deliv. Sci. Technol.* 56, 101556. <https://doi.org/10.1016/j.jddst.2020.101556>.
- Gamal, A., Saeed, H., El-Ela, F.I.A., Salem, H.F., 2021. Improving the antitumor activity and bioavailability of sonidegib for the treatment of skin cancer. *Pharmaceutics* 13 (10), 1560. <https://doi.org/10.3390/pharmaceutics13101560>.
- Gamal, A., Aboelhadid, S.M., Abo El-Ela, F.I., Abdel-Baki, A.-A.S., Ibrahim, S.M., El-Mallah, A.M., Gadelhaq, S.M., 2023. Synthesis of carvacrol-loaded invasomes nanoparticles improved acaricide efficacy, cuticle invasion and inhibition of acetylcholinesterase against hard ticks. *Microorganisms* 11 (3), 733. <https://doi.org/10.3390/microorganisms11030733>.
- Ghasemi, A., Jeddi, S., 2023. Streptozotocin as a tool for induction of rat models of diabetes: a practical guide. *EXCLI J.* 22, 274. <https://doi.org/10.17179/excli2022-5720>.
- Hadaegh, F., Mohebi, R., Cheraghi, L., Tohidi, M., Moghaddam, N.B., Bozorogmanesh, M., Azizi, F., 2012. Do different metabolic syndrome definitions predict cerebrovascular events and coronary heart disease independent of their components? 9 years follow-up of the Tehran lipid and glucose study. *Stroke* 43 (6), 1669–1671. <https://doi.org/10.1161/STROKEAHA.112.650812>.
- Hägg-Holmberg, S., Dahlström, E.H., Forsblom, C.M., Harjutsalo, V., Liebkind, R., Putaala, J., Group, F. S., 2019. The role of blood pressure in risk of ischemic and hemorrhagic stroke in type 1 diabetes. *Cardiovasc. Diabetol.* 18, 1–9. <https://doi.org/10.1186/s12933-019-0891-4>.
- Hamzeloo, M.M., Taiebi, N., Mosaddegh, M., Eslami, T.B., Esmacili, S., 2014. The effect of some cosolvents and surfactants on viability of cancerous cell lines. *Res. J. Pharmacogn.* 1 (3), 41–45.
- Holmberg, B., Malmfors, T., 1974. The cytotoxicity of some organic solvents. *Environ. Res.* 7 (2), 183–192. [https://doi.org/10.1016/0013-9351\(74\)90149-2](https://doi.org/10.1016/0013-9351(74)90149-2).
- Ilieva, Y., Dimitrova, L., Zaharieva, M.M., Kaleva, M., Alov, P., Tsakovska, I., Pajeva, I., 2021. Cytotoxicity and microbicidal activity of commonly used organic solvents: a comparative study and application to a standardized extract from *Vaccinium macrocarpon*. *Toxics* 9 (5), 92. <https://doi.org/10.3390/toxics9050092>.
- Khawaja, Z., Wilcox, C.S., 2011. An overview of candesartan in clinical practice. *Expert. Rev. Cardiovasc. Ther.* 9 (8), 975–982. <https://doi.org/10.1586/erc.11.90>.
- Kozak, A., Ergul, A., El-Remessy, A.B., Johnson, M.H., Machado, L.S., Elewa, H.F., Fagan, S.C., 2009. Candesartan augments ischemia-induced proangiogenic state and results in sustained improvement after stroke. *Stroke* 40 (5), 1870–1876. <https://doi.org/10.1161/STROKEAHA.108.537225>.
- Kumar, R., Salwe, K.J., Kumarappan, M., 2017. Evaluation of antioxidant, hypolipidemic, and antiatherogenic property of lycopene and astaxanthin in atherosclerosis-induced rats. *Pharm. Res.* 9 (2), 161. <https://doi.org/10.4103/0974-8490.204654>.
- Lachenmeier, D.W., 2008. Safety evaluation of topical applications of ethanol on the skin and inside the oral cavity. *J. Occup. Med. Toxicol.* 3, 1–16. <https://doi.org/10.1186/1745-6673-3-26>.
- Lawes, C.M., Bennett, D.A., Feigin, V.L., Rodgers, A., 2004. Blood pressure and stroke: an overview of published reviews. *Stroke* 35 (3), 776–785. <https://doi.org/10.1161/01.STR.0000116869.64771.5A>.
- Li, G., Fan, Y., Fan, C., Li, X., Wang, X., Li, M., Liu, Y., 2012. Tacrolimus-loaded ethosomes: physicochemical characterization and in vivo evaluation. *Eur. J. Pharm. Biopharm.* 82 (1), 49–57. <https://doi.org/10.1016/j.ejpb.2012.05.011>.
- Li, D., Dai, W., Cai, Y., Han, Y., Yao, G., Chen, H., Zhao, X., 2018. Atherosclerosis in stroke-related vascular beds and stroke risk: a 3-D MR vessel wall imaging study. *Ann. Clin. Transl. Neurol.* 5 (12), 1599–1610. <https://doi.org/10.1002/acn3.673>.
- Lian, N., Tong, J., Li, W., Wu, J., Li, Y., 2018. Ginkgetin ameliorates experimental atherosclerosis in rats. *Biomed. Pharmacother.* 102, 510–516. <https://doi.org/10.1016/j.biopha.2018.03.107>.
- Manconi, M., Mura, S., Sinico, C., Fadda, A., Vila, A., Molina, F., 2009. Development and characterization of liposomes containing glycols as carriers for diclofenac. *Colloids Surf. A Physicochem. Eng. Asp.* 342 (1–3), 53–58. <https://doi.org/10.1016/j.colsurfa.2009.04.006>.
- Mosenzon, O., Cheng, A.Y., Rabinstein, A.A., Sacco, S., 2023. Diabetes and stroke: what are the connections? *J. Stroke* 25 (1), 26–38. <https://doi.org/10.5853/jos.2022.02306>.
- Nakao, K., Hirata, M., Oba, K., Yasuno, S., Ueshima, K., Fujimoto, A., Saruta, T., 2010. Role of diabetes and obesity in outcomes of the candesartan antihypertensive survival evaluation in Japan (CASE-J) trial. *Hypertens. Res.* 33 (6), 600–606. <https://doi.org/10.1038/hr.2010.38>.
- Nishimura, Y., Ito, T., Saavedra, J.M., 2000. Angiotensin II AT1 blockade normalizes cerebrovascular autoregulation and reduces cerebral ischemia in spontaneously hypertensive rats. *Stroke* 31 (10), 2478–2486. <https://doi.org/10.1161/01.STR.31.10.2478>.
- Pérez-Corredor, P., Gutiérrez-Vargas, J., Ciro-Ramírez, L., Balcazar, N., Cardona-Gómez, G., 2022. High fructose diet-induced obesity worsens post-ischemic brain injury in the hippocampus of female rats. *Nutr. Neurosci.* 25 (1), 122–136. <https://doi.org/10.1080/1028415X.2020.1724453>.

- Policardo, L., Seghieri, G., Francesconi, P., Anichini, R., Franconi, F., Seghieri, C., Del Prato, S., 2015. Gender difference in diabetes-associated risk of first-ever and recurrent ischemic stroke. *J. Diabetes Complicat.* 29 (5), 713–717. <https://doi.org/10.1016/j.jdiacomp.2014.12.008>.
- Porwal, M., Khan, N.A., Maheshwari, K.K., 2017. Evaluation of acute and subacute oral toxicity induced by ethanolic extract of *Marsdenia tenacissima* leaves in experimental rats. *Sci. Pharm.* 85 (3), 29. <https://doi.org/10.3390/scipharm85030029>.
- Salem, H.F., Gamal, A., Saeed, H., Tulbah, A.S., 2021. The impact of improving dermal permeation on the efficacy and targeting of liposome nanoparticles as a potential treatment for breast cancer. *Pharmaceutics* 13 (10), 1633. <https://doi.org/10.3390/pharmaceutics13101633>.
- Salem, H.F., Gamal, A., Saeed, H., Kamal, M., Tulbah, A.S., 2022. Enhancing the bioavailability and efficacy of Vismodegib for the control of skin cancer: in vitro and in vivo studies. *Pharmaceutics* 15 (2), 126. <https://doi.org/10.3390/ph15020126>.
- Saxena, V., Gacchina Johnson, C., Negussie, A.H., Sharma, K.V., Dreher, M.R., Wood, B. J., 2015. Temperature-sensitive liposome-mediated delivery of thrombolytic agents. *Int. J. Hyperth.* 31 (1), 67–73. <https://doi.org/10.3109/02656736.2014.991428>.
- Sayed, O.M., Abo El-Ela, F.I., Kharshoum, R.M., Salem, H.F., 2020. Treatment of basal cell carcinoma via binary ethosomes of vismodegib: in vitro and in vivo studies. *AAPS PharmSciTech* 21, 1–11. <https://doi.org/10.1208/s12249-019-1574-x>.
- Sezgin-Bayindir, Z., Antep, M.N., Yuksel, N., 2015. Development and characterization of mixed niosomes for oral delivery using candesartan cilexetil as a model poorly water-soluble drug. *AAPS PharmSciTech* 16, 108–117. <https://doi.org/10.1208/s12249-014-0213-9>.
- Shen, L.-N., Zhang, Y.-T., Wang, Q., Xu, L., Feng, N.-P., 2014. Enhanced in vitro and in vivo skin deposition of apigenin delivered using ethosomes. *Int. J. Pharm.* 460 (1–2), 280–288. <https://doi.org/10.1016/j.ijpharm.2013.11.017>.
- Tabassum, R., Vaibhav, K., Shrivastava, P., Khan, A., Ejaz Ahmed, M., Javed, H., Safhi, M.M., 2013. *Centella asiatica* attenuates the neurobehavioral, neurochemical and histological changes in transient focal middle cerebral artery occlusion rats. *Neurol. Sci.* 34, 925–933. <https://doi.org/10.1007/s10072-012-1163-1>.
- Toutitou, E., Dayan, N., Bergelson, L., Godin, B., Eliaz, M., 2000. Ethosomes—novel vesicular carriers for enhanced delivery: characterization and skin penetration properties. *J. Control. Release* 65 (3), 403–418. [https://doi.org/10.1016/S0168-3659\(99\)00222-9](https://doi.org/10.1016/S0168-3659(99)00222-9).
- Tuttolomondo, A., Maida, C., Maugeri, R., Iacopino, G., Pinto, A., 2015. Relationship between diabetes and ischemic stroke: analysis of diabetes-related risk factors for stroke and of specific patterns of stroke associated with diabetes mellitus. *J. Diabetes Metab.* 6 (05), 544–551. <https://doi.org/10.4172/2155-6156.1000544>.
- Vannucci, S.J., Willing, L.B., Goto, S., Alkayed, N.J., Brucklacher, R.M., Wood, T.L., Simpson, I.A., 2001. Experimental stroke in the female diabetic, db/db, mouse. *J. Cereb. Blood Flow Metab.* 21 (1), 52–60. <https://doi.org/10.1097/00004647-200101000-0000>.
- Wang, X., Liu, G., Ma, J., Guo, S., Gao, L., Jia, Y., Zhang, Q., 2013. In situ gel-forming system: an attractive alternative for nasal drug delivery. *Crit. Rev. Ther. Drug Carrier Syst.* 30 (5), 411–434. <https://doi.org/10.1615/CritRevTherDrugCarrierSyst.2013007362>.
- Wouters, K., Shiri-Sverdlow, R., van Gorp, P.J., van Bilsen, M., Hofker, M.H., 2005. Understanding hyperlipidemia and atherosclerosis: lessons from genetically modified apoE and ldlr mice. *Clin. Chem. Lab. Med.* 43 (5), 470–479. <https://doi.org/10.1515/CCLM.2005.085>.
- Xu, W., Deng, Z., Xiang, Y., Zhu, D., Yi, D., Mo, Y., Wan, B., 2022. Preparation, characterization and pharmacokinetics of tolfenamic acid-loaded solid lipid nanoparticles. *Pharmaceutics* 14 (9), 1929. <https://doi.org/10.3390/pharmaceutics14091929>.
- Zhang, Z., Gao, F., Bu, H., Xiao, J., Li, Y., 2012a. Solid lipid nanoparticles loading candesartan cilexetil enhance oral bioavailability: in vitro characteristics and absorption mechanism in rats. *Nanomedicine* 8 (5), 740–747. <https://doi.org/10.1016/j.nano.2011.08.016>.
- Zhang, J.-P., Wei, Y.-H., Zhou, Y., Li, Y.-Q., Wu, X.-A., 2012b. Ethosomes, binary ethosomes and transfersomes of terbinafine hydrochloride: a comparative study. *Arch. Pharm. Res.* 35, 109–117. <https://doi.org/10.1007/s12272-012-0112-0>.
- Zhao, Y., Jiang, Y., Lv, W., Wang, Z., Lv, L., Wang, B., Sun, W., 2016. Dual targeted nanocarrier for brain ischemic stroke treatment. *J. Control. Release* 233, 64–71. <https://doi.org/10.1016/j.jconrel.2016.04.038>.
- Zhao, Y., Li, D., Zhu, Z., Sun, Y., 2020. Improved neuroprotective effects of gallic acid-loaded chitosan nanoparticles against ischemic stroke. *Rejuvenation Res.* 23 (4), 284–292. <https://doi.org/10.1089/rej.2019.2230>.
- Zhou, J., Pavel, J., Macova, M., Yu, Z.-X., Imboden, H., Ge, L., Saavedra, J.M., 2006. AT1 receptor blockade regulates the local angiotensin II system in cerebral microvessels from spontaneously hypertensive rats. *Stroke* 37 (5), 1271–1276. <https://doi.org/10.1161/01.STR.0000217404.64352.d7>.
- Zsuga, J., Gesztelyi, R., Kemeny-Beke, A., Fekete, K., Mihalka, L., Adrienn, S.M., Bereczki, D., 2012. Different effect of hyperglycemia on stroke outcome in non-diabetic and diabetic patients—a cohort study. *Neurol. Res.* 34 (1), 72–79. <https://doi.org/10.1179/1743132811Y.0000000062>.